

Darryl Tchokogoué

ENSTA Paris - Institut Polytechnique de Paris,
828 Boulevard des Maréchaux,
91762 Palaiseau Cedex, France
e-mail: darryl.tchokogoue@ensta.org

Ming Mu

Department of Mechanical Engineering,
Michigan State Technology,
East Lansing, MI 48824
e-mail: ming.mu408@gmail.com

Brian F. Feeny

Professor
Fellow ASME
Department of Mechanical Engineering,
Michigan State Technology,
East Lansing, MI 48824
e-mail: feeny@egr.msu.edu

Bruce K. Geist

Adjunct Associate Professor
Oakland University, Technical Fellow,
FCA US LLC (retired),
Rochester, MI 48309
e-mail: brucegeist@oakland.edu

Steven W. Shaw²

Harris Professor
Fellow ASME
Department of Mechanical, and Civil Engineering,
Florida Institute of Technology,
Melbourne, FL 32901
e-mail: sshaw@fit.edu

The Effects of Gravity on the Response of Centrifugal Pendulum Vibration Absorbers¹

This article describes the effects of gravity on the response of systems of identical, cyclically arranged, centrifugal pendulum vibration absorbers (CPVAs) fitted to a rotor spinning about a vertical axis. CPVAs are passive devices composed of movable masses suspended on a rotor, suspended such that they reduce torsional vibrations at a given engine order. Gravitational effects acting on the absorbers can be important for systems spinning at relatively low rotation speeds, for example, during engine idle conditions. The main goal of this study is to predict the response of a CPVA/rotor system in the presence of gravity. A linearized model that includes the effects of gravity and an order n torque acting on the rotor is analyzed by exploiting the cyclic symmetry of the system. The results show that a system of N absorbers responds in one or more groups, where the absorbers in each group have identical waveforms but shifted phases. The nature of the waveforms can have a limiting effect on the absorber operating envelope. The number of groups is shown to depend on the engine order n and the ratio N/n . It is also shown that there are special resonant effects if the engine order is $n=1$ or $n=2$, the latter of which is particularly important in applications. In these cases, the response of the absorbers has a complicated dependence on the relative levels of the applied torque and gravity. In addition, it is shown that for $N > 1$, the rotor response is not affected by gravity, at least to leading order, due to the cyclic symmetry of the gravity effects. The linear model and the attendant analytical predictions are verified by numerical simulations of the full nonlinear equations of motion.

[DOI: 10.1115/1.4051030]

Keywords: machine dynamics, mechanical signatures, rotor dynamics

1 Introduction

Torsional vibrations represent one of the major issues in power transmission in rotating systems such as shafts and couplings. These torsional vibrations are usually transmitted to the other components of the vehicle or machine to which the engine is linked and therefore can affect the performance and robustness of those components, for example, by producing noise or leading to system failure. Ideally, the torque will be generated and transmitted “smoothly” throughout the entire system. However, in many applications, including aerospace and automotive systems, the torque has fluctuations for which the excitation frequency is proportional to the mean rotation rate of the engine, via a constant known as the engine order, denoted here as n . A common example is internal combustion engines for which the cylinder gas pressure varies significantly over each cycle, leading to engine order torsional loading. In particular, for four-stroke engines, the dominant engine excitation order is one-half the number of cylinders, since each cylinder fires once per two revolutions of the crank. In multi-cylinder engines, this harmonic is generally much larger than higher order harmonics.

There are several means of reducing torsional vibrations. A method that has been around for nearly a century, and has recently become popular in automotive applications, is to use centrifugal pendulum vibration absorbers (CPVAs). These absorbers allow

for smooth operation that offers improved fuel economy in automotive engines, for example, by widening operating conditions for torque converter lockup [1,2].

A CPVA does not require any external energy supply and acts as a passive device. The restoring force on a centrifugal pendulum is provided by centrifugal effects induced by the rotor, so that the natural frequency of a CPVA is proportional to the mean rotating speed of the rotor, thereby offering engine order tuning. The key parameters for absorber design are its tuning order, which is set by the geometry and inertia of the absorber and its effective rotational mass about the rotor center. The absorber order is the ratio of pendulum frequency to mean rotor speed, which depends on the geometry of the CPVA and its suspension; this arrangement allows it to be tuned relative to the engine order. Also, it is important to note that, due to balancing issues, CPVAs are commonly distributed in a cyclic manner about the spinning rotor, a feature exploited in the present analysis, where we consider systems with N identical, cyclically arranged absorbers.

The implementation of CPVAs in automotive engines results in a horizontal rotation axis, so that the CPVAs can be influenced by gravity, which is an excitation of engine order one. The response of the absorbers (and rotor) is a combination of two effects, of orders n from the applied torque and order one from gravity. In typical engines, gravity will be important only at low engine speeds, specifically such that g is 5% or more of the rotor centrifugal effects that act on the absorbers, which is around typical idle speeds [3]. The order n component of the response of a set of identical absorbers is generally synchronous since the order n excitation comes from rotor angular acceleration and acts identically on all absorbers. In contrast, the order one excitation from gravity results in a response component that is cyclically phase shifted

¹This article is dedicated to the memory of Victor J. Borowski, whose enthusiasm about pendulum absorbers continues to inspire our work on this important subject.

²Corresponding author.

Contributed by the Technical Committee on Vibration and Sound of ASME for publication in the JOURNAL OF VIBRATION AND ACOUSTICS. Manuscript received October 8, 2020; final manuscript received March 23, 2021; published online May 25, 2021. Assoc. Editor: Shahrzad Towfighian.

among the absorbers. The combination leads to absorbers that can have distinct motions in amplitude and/or phase. This lack of synchronous behavior among identical absorbers is known to be an issue in their design since some absorbers may reach their amplitude limits before others.

In addition to gravity, nonsynchronous responses among identical absorbers can also result from dynamic instabilities related to nonlinear inertial coupling among the absorbers [4–6]. Remedies to the nonsynchronous problem include designs, which kinematically lock the absorbers to one another, enforcing synchronicity [7], and designs with springs between adjacent absorbers that can suppress, but not eliminate, asynchronicity [8]. However, for simple, standard bifilar designs, the asynchronous behavior presented in this study will be present and can be important at low engine speeds.

Investigations on the effects of gravity on the dynamics of CPVA systems with multiple absorbers have been carried out by Theisen [3], Shi et al. [9], and Mu [10]. Theisen investigated the nonlinear response of CPVAs with gravity using perturbation methods and simulations, and Shi and Mu considered their linear response using symmetry properties and simulations. The current work is based primarily on Ref. [10] but has additional important generalizations to all previous studies. The previous studies showed that the absorbers would respond in a complicated manner that depends in a nontrivial way on n and N . Three types of response conditions were observed: (i) the absorbers all act identically with different phases related to their position on the rotor; (ii) the absorbers arrange into two or more groups with each group having identical, but phase shifted, waveforms; and (iii) each absorber has a unique response waveform. In the present investigation, this grouping behavior is studied from a general point of view using the symmetry properties of the system. Also, the previous studies are interested in only the case where the engine order is strictly greater than 1 and do not consider a general number of absorbers N . The present results cover all realistic values of the engine orders for systems with an arbitrary N , and a general result is obtained that allows one to predict the absorber grouping properties. Much of the development and background work can be found in Refs. [3,9,10], but this study, which is carried out in a more systematic manner, contains new results about the grouping of absorbers, sheds light on the special resonant interactions that occur for engine orders one and two, and provides useful analytical predictions for the response of the absorbers and the rotor.

Gravity provides both direct and parametric excitation to the CPVAs. Such systems have been studied in the context of parametric amplification, which also have both direct and parametric excitation, but differ in a significant way since the frequency of the parametric excitation is always at (or near) twice that of the direct excitation [11,12]. Such a situation for CPVAs applies only in the case $n = 1/2$, which is not important for CPVAs in automotive engines. A system with similar gravity-driven dynamics is that of a wind-turbine blade vibrations coupled through the rotor hub. One difference between that system and the CPVA system is that the wind turbines are excited through direct loading on the blades rather than a torque on the rotor, such that the direct excitation on the blades does not have a common phase. Acar et al. [13] studied in-plane wind-turbine blade vibrations coupled through the rotor for very large turbines with identical blades. That study involved a combination of parametric and direct excitations at the same order and presented an analysis of superharmonic resonances of order two on the blades and the resulting rotor oscillations. In that case, with three blades and order one parametric and direct excitation, the three blades had the same response, although phase shifted. In a follow-up study, Sapmaz et al. [14] looked at how blade mistuning disrupted the uniformity of the blade responses and considered superharmonics of order three by using a second-order multiple-scale analysis [15] and also examined an occurrence of speed locking [16] due to blade resonance. Ikeda et al. [17] studied out-of-plane nonlinear vibration of three parametrically excited rotating blades coupled through the hub moving in the horizontal plane on the top of the tower. They also considered vibration localization and instability conditions. Also, in another relevant

study, primary resonance and superharmonic resonances of single degree-of-freedom systems with direct and parametric excitation at the same excitation frequency were studied using the method of multiple scales (MMS) [18]. It was found that for primary resonance, a first-order MMS analysis did not reveal a contribution from the parametric terms, but a second-order MMS analysis uncovered a parametric amplification. The characteristics of this parametric amplification had some similarities with that of Ref. [12], although it occurred in the subharmonic parametric wedge rather than at primary resonance. Superharmonic resonances of order two were also studied by a first-order MMS [19] and by the method of van der Pol [20], and superharmonic resonances of order three in the linearized system were studied by a second-order MMS [18]. However, in that case, the off-primary case does not involve any effect equivalent to the first-order gravity term.

This article considers the response of CPVA systems in gravity, focusing on the resulting waveforms of the absorbers and possible grouping properties and resonances that can arise with different numbers of absorbers and torque excitation orders. It is shown that for $n \neq 1, 2$, the response is described by a relatively simple linear time-invariant system with direct excitation from gravity and the applied torque. However, it is shown that in the $n = 1, 2$ resonant cases, gravity has a nontrivial effect on the response of the absorbers due to the gravitational parametric excitation. The rotor response is also considered in this study, although we do not focus on the performance of the absorbers in terms of reducing torsional vibrations, as that topic has been extensively covered in the literature, compared with Refs. [5,6,21]. In fact, it will be seen that gravity has, to leading order, no effect on the rotor response for $N > 1$ absorber systems with cyclic symmetry, when the absorber responses follow that symmetry. For a single absorber $N = 1$, gravity has a dramatic effect on the rotor, and this case is considered. Also, it is noted that when the absorbers are operating as desired, they reduce the order n harmonic component of the rotor response. In fact, this often leads to a situation where higher order, nonlinear effects result in rotor vibration harmonics of orders $2n$ and $3n$ that are comparable, or even larger, than the order n component [21–23]. Since the present linear analysis ignores these higher harmonics, simulations of the rotor response from the full nonlinear equations of motion (EOM) may differ from the present predictions, even when the absorber responses are accurately captured by the linear analysis.

This article is arranged as follows: Sec. 2 outlines the governing equations of motion and their nondimensionalization and linearization, resulting in a model with both direct and parametric excitation acting on the absorbers. In Sec. 3, we carry out a perturbation analysis of the equations of motion to determine the system steady-state response. Our approach takes advantage of the cyclic properties of the equations of motion, which reveals their important features. Section 4 describes the main results and demonstrates them using some representative examples, and this article closes with a discussion in Sec. 5.

2 Modeling

2.1 Assumptions. The model to be investigated consists of a rigid rotor rotating about a fixed axis that is perpendicular to gravity. Note that by Einstein's equivalence principle, this analysis also applies to a situation in which the system is accelerated in any direction perpendicular to the rotor axis, for example, the forward acceleration of a car with a transversely mounted engine. The rotor is subjected to a harmonic torque of order n and is assumed to spin with periodic fluctuations about a mean rate Ω . The N absorbers are identical and cyclically arranged around the rotor. They are modeled as point masses that move along paths relative to the rotor, prescribed by design so that the absorber order is \tilde{n} , which is close to n by design. (The point mass assumption is valid for absorbers with bifilar suspensions and negligible inertia of the support pins.) The rotor angle is expressed as θ and the

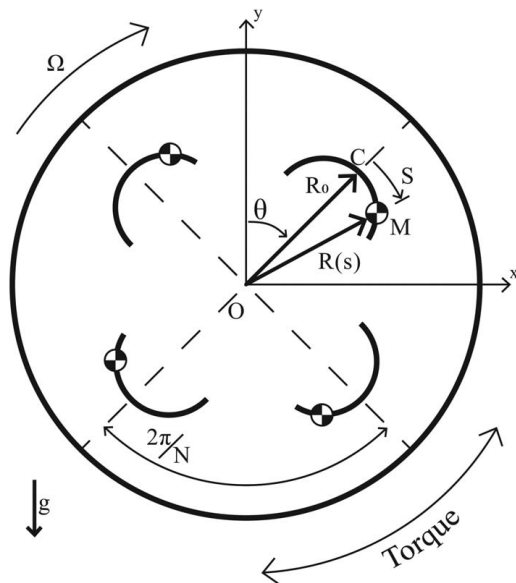


Fig. 1 Layout of a rotor with $N = 4$ absorbers with details shown for a single absorber

absorber positions are denoted by S_j , $j = 1, \dots, N$, the arc lengths along their paths, taken to be zero at their central positions, i.e., the path vertices. We assume that the absorbers and rotor are linearly damped. It will be assumed that all absorbers are geometrically and materially identical, that is, $m_{pj} = M$ and all path parameters are the same. However, the absorbers generally have distinct displacements during the system response, so we do not assume that the absorber positions S_j 's are equal.

Since the absorbers are cyclically placed around the rotor, the angle indicating the location of absorber j on the rotor is thus given by $\theta_j = \theta + \phi_j$, where $\phi_j = 2\pi(j-1)/N$ is the sector angle of θ_j relative to θ , which points to the vertex of the path of absorber j . Figure 1 depicts a schematic of this layout, showing four absorbers and the cyclic sector layout.

2.2 Equation of Motion. Figure 1 shows details for one of the N absorbers to specify their important features. The symbols used in this figure are listed in Table 1, along with their physical descriptions. The generalized coordinates for the dynamic model are taken to be θ and S_j , $j = 1, \dots, N$. The rotor has the moment of inertia J_{rot} , and the j th absorber has mass $m_{pj} = M$.

The fluctuating torque acting on the rotor, from, for example, cylinder gas pressure, is modeled as $T_0 + T_\theta \sin(n\theta + \tau)$, where T_0 is the mean torque, T_θ is the amplitude of the fluctuating torque at order n (the engine order), and τ is a phase needed to define the phase of the harmonic torque relative to the rotor orientation (θ), that is, relative to gravity. This torque results in (relatively

Table 1 Symbols and descriptions for Fig. 1

Symbols	Description
O	Center of rotor
C	Center of the absorber path—its vertex
R_0	Distance between O and C
S	Arc length position of absorber mass
$R(S)$	Distance between O and the absorber at S
M	Absorber mass
Ω	Mean rotational speed of rotor
θ	Rotor crank angle
g	Gravity
y	Lab fixed vertical coordinate, in direction of g
x	Lab fixed horizontal coordinate

small) fluctuations of the rotor speed, expressed as $\dot{\theta} - \Omega$, where $\langle \dot{\theta} \rangle = \Omega$ is the mean rotor speed, which is assumed to be constant.

The EOM of the system are obtained using Lagrange's equations, as described, for example, in Ref. [24], where the effects of gravity are included by using the associated potential energy [3,10]. The rotor EOM is given by

$$J_{rot}\ddot{\theta} + \sum_{j=1}^N m_{pj} \left[R^2(S_j)\ddot{\theta} + \frac{dR^2(S_j)}{dS}\dot{S}_j\dot{\theta} + G(S_j)\ddot{S}_j + \frac{dG(S_j)}{dS}\dot{S}_j^2 - g(X_p(S_j)\cos(\theta_j) + Y_p(S_j)\sin(\theta_j)) \right] = -c_0\dot{\theta} + T_0 + T_\theta \sin(n\theta + \tau)$$

and the EOM for the j th absorber is expressed as follows:

$$m_{pj} \left[\ddot{S}_j + G(S_j)\ddot{\theta} - \frac{1}{2} \frac{dR^2(S_j)}{dS}\dot{\theta}^2 + g \left(-\frac{dX_p(S_j)}{dS}\sin(\theta_j) + \frac{dY_p(S_j)}{dS}\cos(\theta_j) \right) \right] = -c_{aj}\dot{S}_j$$

where X_p and Y_p are the x and y components of the location of the center of mass of m_{pj} relative to O , c_0 is the damping coefficient of the rotor, and c_{aj} is the damping coefficient for the j th absorber. The function $G(S_j)$ appears in the kinetic energy as a result of the motion of the absorber along its path and is given by

$$G(S_j) = R(S_j) \sqrt{1 - \left(\frac{dR(S_j)}{dS} \right)^2}$$

It represents a product of the radial distance $R(S_j)$ and the cosine of the angle between a unit vector tangent to the path and another that is perpendicular to the radial line \overline{OC} in Fig. 1. The term $G(S_j)\ddot{\theta}$ in the S_j equation dictates the level of base excitation from the rotor angular acceleration onto the absorber, as well as the coupling of the absorber motion back onto the rotor. These equations are fully nonlinear and are to be nondimensionalized and linearized for the present investigation.

2.3 Nondimensionalization and Linearization. To linearize the EOM, one must specify the path of the absorber near its vertex, as determined by the function $R(S)$, which then dictates $X(S)$, $Y(S)$, and $G(S)$. A general family of epicycloidal paths that includes the important cases of circular and tautochronic paths will be considered here, the details for which are given in Table 2 as functions of the arc length variable S [6,24]. Here, ρ_0 is the path radius of curvature at the vertex ($S=0$) (essentially, the effective absorber pendulum length), $\lambda \in [0,1]$ is a characteristic parameter dictating the nonlinear nature of the path, and the angle Φ_j is the angular position of absorber j from its vertex, given by $\Phi_j = (1/\lambda) \arcsin(\lambda(S_j/\rho_0))$ [24]. Upon linearization, these simplify considerably, and λ will drop out of the present formulation. For simulations of the full equations of motion, we employ the tautochronic epicycloidal path with $\lambda = \tilde{n}/\sqrt{1 + \tilde{n}^2}$, since it minimizes nonlinear frequency shifts over the largest possible range of absorber motions [24].

Note that the radius of curvature ρ_0 dictates the small amplitude (linear) absorber tuning order, \tilde{n} , which is purely geometry dependent and governed by the relation:

$$\rho_0 = \frac{R_0}{\tilde{n}^2 + 1}$$

where \tilde{n} is the small amplitude absorber tuning. This can be shown to be equal to the square root of the ratio of the distance from O to the effective pendulum support point to the effective pendulum length.

Table 2 Nonlinear path functions from Ref. [24] and their expanded forms for the tautochronic epicycloidal path tuned to order \tilde{n} with terms up to second-order in $s_j = S_j/R_0$ retained

Term	Nonlinear expressions from Ref. [24]	Expanded form in terms of s_j
$X_p(S_j)$	$\frac{\rho_0}{1-\lambda^2}(\sin(\Phi_j)\cos(\lambda\Phi_j) - \frac{\lambda^2 S_j}{\rho_0}\cos(\Phi_j))$	$R_0 s_j$
$Y_p(S_j)$	$R_0 + \frac{\rho_0}{1-\lambda^2}(\cos(\Phi_j)\cos(\lambda\Phi_j) + \frac{\lambda^2 S_j}{\rho_0}\sin(\Phi_j) - 1)$	$R_0\left(1 - \frac{1}{2}(1 + \tilde{n}^2)s_j^2\right)$
$R^2(S_j)$	$X_p^2 + Y_p^2$	$R_0^2(1 - \tilde{n}^2 s_j^2)$
$G(S_j)$	$R(S_j)\sqrt{1 - \left(\frac{dR(S_j)}{dS_j}\right)^2}$	$R_0\left(1 - \frac{1}{2}\tilde{n}^2 s_j^2\right)$

The nondimensionalization is carried out by rescaling variables and functions, as follows:

- (i) The normalized absorber displacement is defined by $s_j = S_j/R_0$, where $|s_j| < 1/\tilde{n}\sqrt{1 + \tilde{n}^2} (< 1)$ for epicycloidal paths (determined by the limits where $G(s_j)$ is real [6]). Therefore, terms that depend on s_j can be expanded in Taylor series about $s_j=0$. Linear terms in s_j are retained in the EOM. Note that quadratic terms are required for some terms in the path functions since derivatives of these functions appear in the EOM.
- (ii) The normalized rotating speed fluctuation is defined by $\omega = (\dot{\theta}/\Omega) - 1$, where $|\omega| \ll 1$, that is, the speed fluctuations are small compared to Ω , for realistic operating conditions. Note that the mean rotor speed is, to leading order, set by a balance of the mean rotor torque and the rotor damping, i.e., $\langle \dot{\theta} \rangle = \Omega = T_0/c_0$.
- (iii) The independent variable is changed from time t to the rotor angle θ . This converts the applied torque and the gravity loads, which depend on θ , to harmonic forcing terms of the usual form. By using the chain rule, it is seen that $d(\cdot)/dt = \dot{\theta} (d(\cdot)/d\theta) = \dot{\theta}(\cdot)'$ and $d^2(\cdot)/dt^2 = \ddot{\theta}(\cdot)'' + \dot{\theta}^2(\cdot)''$, where $(\cdot)'$ denotes the derivative with respect to θ . Interestingly, for the rotor angular speed and acceleration, this conversion yields $\dot{\theta} = \Omega(1 + \omega(\theta))$ and $\ddot{\theta} = \Omega^2 \omega'(\theta)(1 + \omega(\theta))$. This transformation is valid so long as $\dot{\theta}$ is never zero, as is the case in for our steady-state analysis with small speed fluctuations about Ω .
- (iv) Dimensionless system parameters are formulated as follows:
 - $\nu = NMR_0^2/J_{rot}$ is the ratio of total absorber inertia to the rotor inertia.
 - $\Gamma_\theta = T_\theta/J_{rot}\Omega^2$ is the fluctuating torque level normalized by twice the kinetic energy of the rotor.
 - $\gamma = g/R_0\Omega^2$ is gravity normalized by the centrifugal acceleration of the absorber vertex.
 - $\mu_a = c_a/m\Omega$ is the nondimensional absorber damping coefficient.

Note that all these parameters are small in practice.

The full nonlinear equations for $\omega(\theta)$ and $s_j(\theta)$ can be found in, for example, Ref. [6], for the case without gravity. Inclusion of the gravity terms is described in Ref. [9] and can be expressed in terms of the variables described herein. The fully nonlinear equations expressed in a dimensionless form are used to derive the linearized equations presented below and for verification by numerical simulations in Sec. 4.

The linearization of the equations of motion is carried out by an expansion that retains only first-order terms in the s_j 's and ω . The resulting rotor equation can be solved for ω' , resulting in

$$\omega' = \frac{1}{1 + \nu} \left[\Gamma_\theta \sin(n\theta + \tau) - \frac{\nu}{N} \sum_{j=1}^N s_j'' \right] \quad (1)$$

where in this expression, we have ignored terms of the form $\nu\gamma s_j$ since these terms are of higher order and have a negligible effect on the analytical results. Here, it is seen that the rotor angular acceleration is a combination of the effects of the applied torque and the sum of the absorber actions on the rotor. Also, note that only orders 1 and n will be captured by this expression and, as noted earlier, nonlinear effects can result in significant amplitudes at larger harmonics, especially in the rotor response [21]. Also note that if one locks the absorbers, a situation used to determine the effectiveness of the absorbers' dynamics in reducing rotor vibrations, the s_j'' terms are zero and one can use the resulting version of Eq. (1) for the baseline rotor angular acceleration. The mathematical view of the absorbers' effect on the rotor is that when they are operating as desired, the summed s_j'' terms in ω' , representing the torque applied by the absorbers to the rotor, largely cancel the term arising from the applied torque. Substituting the expression in Eq. (1) into the linearized absorber EOM for the j th absorber allows one to decouple them from the rotor EOM [10,25], resulting in

$$s_j'' + \mu_a s_j' + (\tilde{n}^2 - \gamma(1 + \tilde{n}^2)\cos(\theta_j))s_j = \gamma \sin(\theta_j) - \frac{1}{(1 + \nu)} \left[\Gamma_\theta \sin(n\theta + \tau) + \frac{\nu}{N} \sum_{k=1}^N s_k'' \right] \quad (2)$$

where ν, γ, μ_a , and Γ_θ are generally small, on the order of 0.1 or less, in practice. Note that this form of the equations of motion clearly indicates the global inertial coupling of the absorber dynamics through the rotor. It also shows how gravity drives the absorbers both directly and parametrically through the sector rotor angle θ_j , as expected in such a rotating system.

Since these absorbers are designed specifically to be effective over a wide range of rotor speeds Ω , it is worth commenting on the effects of Ω in light of the nondimensionalized system parameters. The mean rotor speed appears in the gravity parameter γ , the fluctuating torque parameter Γ_θ , and the absorber damping parameter μ_a . In the examples presented later, we take fixed values of γ and μ_a and vary the torque level Γ_θ , corresponding to a test in which the mean rotor speed Ω is kept constant and the fluctuating torque level T_θ is varied. To compare the present results with tests that vary Ω , one must account for its effect on the dimensionless parameters noted earlier. This is discussed in more detail in Sec. 3.4.

In the differential equation for absorber j , the absorber is subjected to order n direct excitation, caused by the rotor angular acceleration (originally from the applied torque at order n), as well as by direct and parametric excitation at order 1 arising from gravity. The order n excitation is equal for all absorbers, since they are connected identically to the rotor, which provides rotational base excitation from the rotor angular acceleration. The order 1 excitations are cyclic in nature since the gravitational forces on absorber j depend on the absorber position on the rotor. Therefore, it can be assumed that the response of the absorbers will have components at order 1, cyclically shifted by index j around the rotor, and order n , which will be identical for all absorbers, plus possible

linear combinations of these from the parametric excitation. Explicit, approximate expressions for these components are derived subsequently.

The nature of the absorber response components leads to some interesting consequences, the first of which is an observation about the rotor response, which depends on the absorber responses; see Eq. (1). When the absorber response components are identical at order n and phase shifted by ϕ_j at order 1, the effects of the absorbers on the rotor at order n add directly, while, for $N > 1$, those of order 1 sum to zero, due to their cyclic nature [26]. This implies that for $N > 1$ gravity has no effect on the rotor response, unless the order n components of the absorbers are affected by gravity, which we show is not the case. The second consequence is the important grouping behavior described in Sec. 2.4.

2.4 Grouping Behavior. As observed in previous studies [3,10], in some cases, the steady-state response of the absorbers is composed of subgroups where some absorbers have equal amplitude but are phase-shifted, and multiple subgroups can occur. To predict how this grouping will occur for a given n and N , it is convenient to express the general form of the response of the j th absorber with an order n component of complex amplitude $2A$ and a cyclic order 1 component of complex amplitude $2B$ as follows:

$$s_j(\theta) = Ae^{i(n\theta+\tau)} + Be^{i\theta_j} + c.c. \quad (3)$$

where τ accounts for the phase shift between the orders, $c.c.$ denotes the complex conjugate of the preceding terms, and, recall that $\theta_j = \theta + (2\pi(j-1)/N)$ is the rotor angle for the position of absorber j . Consider the k th absorber, which is ℓ sections circumferentially away from the j th absorber, so that $k = j + \ell$. The response of this absorber is expressed as follows:

$$s_k(\theta) = Ae^{i(n\theta+\tau)} + Be^{i(\theta_j+2\pi\ell/N)} + c.c. \quad (4)$$

noting that the order n response is the same for all absorbers and that the order one component is phase shifted by the sector angle between the absorbers. Note that this form holds for $\ell = 1, 2, \dots, (N-1)$.

Now consider the conditions under which the waveform of the k th absorber will be identical to that of the j th absorber, but with a different phase. To this end, we add a dummy phase ψ to both components of absorber j and examine the conditions for which $s_k(\theta) = s_j(\theta + \psi)$. The following expansion of $s_j(\theta + \psi)$ is used to compare it with s_k :

$$s_j(\theta + \psi) = Ae^{i(n\theta+n\psi+\tau)} + Be^{i(\theta_j+\psi)} + c.c. \quad (5)$$

Since there are two groups of exponential functions (order 1 and order n) with different orders in the steady-state response of each absorber, to have $s_k(\theta) = s_j(\theta + \psi)$, it is necessary to have $n\psi = 2\pi p$, $p \in \mathbb{Z}$ and $\psi - (2\pi\ell/N) = 2\pi q$, $q \in \mathbb{Z}$, where \mathbb{Z} is the set of integers. The condition for identical absorber waveforms can be expressed by eliminating ψ from these two conditions, resulting in the following condition on ℓ as a function of indices p and q ,

$$\ell = \frac{N}{n}(p - nq) \quad (6)$$

By accounting for the condition that $\ell = 1, 2, \dots, (N-1)$, the grouping behavior for order n torque and N cyclically placed absorbers is summarized in Table 3, by indicating the number of groups that will occur for each case. The rigorous proof for these results is given in the Appendix. Note that Table 3 includes results for four-stroke engines with an odd number of cylinders, for which $2n$ is an integer but n is not an integer. Note that the

Table 3 Summary of grouping properties

$\frac{N}{n}$	n	Number of groups	Shift index	Number of absorbers per group
Integer	Integer	$\frac{N}{n}$	$\frac{N}{n}$	n
Integer	Not integer	$\frac{N}{2n}$	$\frac{N}{2n}$	$2n$
Not integer	Either	N	N	1

number of groups can be N/n , $N/2n$, or N and can range from 1, in which case all absorbers act identically (with phase shifts), to N , where each absorber has a distinct waveform. These general results will be demonstrated by examples after the steady-state responses are analyzed.

Some interesting cases of practical interest include the following: Consider a four-cylinder, four-stroke engine, which has $n = 2$, with N absorbers; this arrangement will result in $N/2$ groups if N is even and N groups if N is odd. Similarly, consider a three-cylinder engine, which has $n = 1.5$, with N absorbers: this arrangement will result in $N/3$ groups if N is a multiple of 3, otherwise all absorbers will act individually, that is, there will be N groups.

3 Steady-State Response

To carry out an analysis of the steady-state responses, even for the linearized model, we require an approximation technique due to the presence of the gravitational parametric excitation effects on the absorbers. Here, we employ the MMS on the linear EOMs by introducing a small parameter, $\hat{\epsilon}$, to be used in the expansions. This method will automatically indicate situations in which resonant effects can occur. The case of order $n = 1$ will require a different scaling from $n \neq 1$, since in that case the gravity term provides direct resonant excitation to the absorbers. It will also be seen that the effects of the parametric excitation come into play only for $n = 2$. For $n \neq 2$, the response is described by expressions that represent straightforward linear vibration analysis. Here, the analysis is facilitated by exploiting the cyclic nature of the equations of motion [26].

3.1 Scaling and Slow Flow Equations. In these absorber systems, practical conditions are well suited for the introduction of a small parameter, and these have guided our choice of nondimensional parameters, as described earlier. Specifically, the absorbers have small inertia when compared to the rotor ($\nu \ll 1$, which implies small interabsorber coupling through the rotor), the absorbers are lightly damped ($\mu_a \ll 1$), and the fluctuating torque is small compared with the rotor kinetic energy ($\Gamma_\theta \ll 1$), resulting in relatively small fluctuations in rotor speed ($\omega \ll 1$), and the travel of the absorbers is small compared to the size of the rotor ($s \ll 1$). These parameters will be scaled by $\hat{\epsilon} \ll 1$ in Eq. (2). We begin with a general scaling and chose specific orders to bring out the physics of interest. Specifically, we let

$$s_j = \hat{\epsilon}^P p_j, \quad \omega = \hat{\epsilon}^W \xi, \quad \nu = \hat{\epsilon}^B \delta, \quad \mu_a = \hat{\epsilon}^L \tilde{\mu}_a, \quad \gamma = \hat{\epsilon}^G \tilde{\gamma}, \quad \Gamma_\theta = \hat{\epsilon}^\Gamma \tilde{\Gamma}_\theta, \quad \tilde{n} = n(1 + \hat{\epsilon}^Q \sigma) \quad (7)$$

and seek exponents that capture the dynamics of interest. The physical meanings of these scaled variables and parameters are as follows: p_j is the absorber displacement, δ is the inertia ratio, $\tilde{\mu}_a$ is the absorber damping, $\tilde{\gamma}$ is the strength of gravity, $\tilde{\Gamma}_\theta$ is the amplitude of the fluctuating torque, and σ is the tuning offset of the absorber relative to the engine order, which is set by design [6,27]. Note that with the use of $\hat{\epsilon}$, we have one free variable so that we can take $\delta = 1$ and define the inertia ratio to be $\hat{\epsilon}^B$. Using this scaling in Eq. (2) and choosing exponents that keep the

parametric excitation term at leading order, along with the other effects of interest, namely, direct excitation, damping, and coupling, one selects $P=L=G=B=Q=1/2$ and $\Gamma=1$. It will be seen that

$$p_j'' + n^2 p_j - \tilde{\gamma} \sin(\theta_j) + \epsilon \left[\tilde{\mu}_a p_j' + \frac{\delta}{N} n^2 \sum_{k=1}^N p_k + (2n^2 \sigma - \tilde{\gamma}(1+n^2) \cos(\theta_j)) p_j + \tilde{\Gamma}_\theta \sin(n\theta + \tau) \right] = 0 \quad (8)$$

Following the standard procedure for the MMS, the absorber response can be expressed as an expansion of p_j :

$$p_j = p_{0j} + \epsilon p_{1j} + \dots$$

where both the p_0 and p_1 depend on "time" (actually, angular displacement) scales $\hat{\theta}_0 = \theta$ and $\hat{\theta}_1 = \epsilon\theta$, where the overhat is used so that these time scales are not confused with the absorber angles θ_j . (Note that the rotor angle here plays the role of time, so that the applied torque appears in the usual manner as a harmonic excitation.)

The equations at order ϵ^0 and ϵ^1 are given by

$$\begin{aligned} \epsilon^0: \quad D_0^2 p_{0j} + n^2 p_{0j} &= \tilde{\gamma} \sin(\hat{\theta}_{j0}) \\ \epsilon^1: \quad D_0^2 p_{1j} + n^2 p_{1j} &= -2D_0 D_1 p_{0j} - \tilde{\mu}_a D_0 p_{0j} - \frac{1}{N} \delta n^2 \sum_{k=1}^N p_{0k} \\ &\quad - [2n^2 \sigma - (1+n^2)\tilde{\gamma} \cos(\hat{\theta}_{j0})] p_{0j} - \tilde{\Gamma}_\theta \sin(n\hat{\theta}_0 + \tau) \end{aligned} \quad (9)$$

where D_0 is the partial derivative respect to the scaled rotor angle $\hat{\theta}_0$, D_1 is the partial derivative with respect to $\hat{\theta}_1$, and $\hat{\theta}_{j0} = \hat{\theta}_0 + \phi_j$.

From the ϵ^0 equation, the solution for p_0 , which includes so-called hard excitation [28], is given by

$$p_{0j} = A_j(\hat{\theta}_1) e^{in\hat{\theta}_0} + \Lambda e^{i\hat{\theta}_{j0}} + c.c. \quad (10)$$

where $\Lambda = \tilde{\gamma}/2i(n^2 - 1)$ captures the order one response to gravity. Here, it is seen that this solution is valid for $n \neq 1$ and that a different scaling is needed for $n=1$, which is investigated subsequently in Sec. 3.3.

By using this solution for p_{0j} in the ϵ^1 equation, the following equation is obtained for p_{1j} :

$$\begin{aligned} \epsilon^1: \quad D_0^2 p_{1j} + n^2 p_{1j} &= -2D_0 D_1 (A_j e^{in\hat{\theta}_0} + \Lambda e^{i(\hat{\theta}_0 + \phi_j)} + c.c.) \\ &\quad - \tilde{\mu}_a D_0 (A_j e^{in\hat{\theta}_0} + \Lambda e^{i(\hat{\theta}_0 + \phi_j)} + c.c.) \\ &\quad - \frac{1}{N} \delta n^2 \sum_{k=1}^N (A_k e^{in\hat{\theta}_0} + \Lambda e^{i(\hat{\theta}_0 + \phi_k)} + c.c.) \\ &\quad - 2n^2 \sigma (A_j e^{in\hat{\theta}_0} + \Lambda e^{i(\hat{\theta}_0 + \phi_j)} + c.c.) \\ &\quad + \frac{1}{2} \tilde{\gamma} (1+n^2) (e^{i(\hat{\theta}_0 + \phi_j)} + e^{-i(\hat{\theta}_0 + \phi_j)}) (A_j e^{in\hat{\theta}_0} + \Lambda e^{i(\hat{\theta}_0 + \phi_j)} + c.c.) \\ &\quad - \frac{1}{2i} \tilde{\Gamma}_\theta (e^{i(n\hat{\theta}_0 + \tau)} - e^{-i(n\hat{\theta}_0 + \tau)}) \end{aligned}$$

In order to obtain a bounded solution as $\hat{\theta}_0$ evolves, secular terms must be eliminated. Here, the secular terms are at order n and depend of the value of n . The possible cases are $n=1$, $n=2$, and $n \neq 1, 2$. Since the system must be rescaled for $n=1$, the analysis following immediately below considers the situations for $n=2$ and $n \neq 1, 2$.

For $n \neq 1, 2$, i.e., nonresonant cases, the elimination of secular terms leads to the following slow flow equation for the complex amplitude A_j of the j th absorber:

$$A_j' + \frac{1}{2} (\tilde{\mu}_a - 2in\sigma) A_j - i \frac{\delta n}{2N} \sum_{k=1}^N A_k = \frac{1}{4n} \tilde{\Gamma}_\theta e^{i\tau} \quad (11)$$

this scaling works for $n \neq 1$ and that another form of the scaling is required for $n=1$. Expanding Eq. (2) and defining $\epsilon = \hat{\epsilon}^{1/2}$ give the leading order absorber equation as follows:

For $n=2$, that is, a superharmonic resonance of order two, the elimination of secular terms yields the following slow flow equation for the amplitude of the j th absorber:

$$A_j' + \frac{1}{2} (\tilde{\mu}_a - 2in\sigma) A_j - i \frac{\delta n}{2N} \sum_{k=1}^N A_k = \frac{1}{4n} \tilde{\Gamma}_\theta e^{i\tau} - i \frac{1}{4n} \tilde{\gamma} (1+n^2) \Lambda e^{i2\phi_j} \quad (12)$$

where A_j is a function of $\hat{\theta}_1$.

Equations (11) and (12) can be written in a matrix form as follows:

$$\mathbf{A}' + \mathbf{K}\mathbf{A} = \mathbf{F}_t + \mathbf{F}_g \quad (13)$$

where \mathbf{A} is the vector of complex amplitudes, \mathbf{F}_t is the forcing from the applied torque, \mathbf{F}_g results from gravity, and the complex stiffness matrix is given by

$$\mathbf{K} = \frac{1}{2} \begin{pmatrix} \tilde{\mu}_a - in \left(2\sigma + \frac{\delta}{N} \right) & -i \frac{\delta n}{N} & \dots & -i \frac{\delta n}{N} \\ -i \frac{\delta n}{N} & \tilde{\mu}_a - in \left(2\sigma + \frac{\delta}{N} \right) & \dots & -i \frac{\delta n}{N} \\ \vdots & \vdots & \ddots & \vdots \\ -i \frac{\delta n}{N} & -i \frac{\delta n}{N} & \dots & \tilde{\mu}_a - in \left(2\sigma + \frac{\delta}{N} \right) \end{pmatrix} \quad (14)$$

and the torque excitation terms are given by

$$\mathbf{F}_t = \frac{\tilde{\Gamma}_\theta}{4n} \begin{pmatrix} 1 \\ 1 \\ \vdots \\ 1 \end{pmatrix} e^{i\tau} \quad (15)$$

For $n \neq 1, 2$ gravity has no effects, that is, $\mathbf{F}_g = \mathbf{0}$, while for $n=2$,

$$\mathbf{F}_g = -\frac{i\tilde{\gamma}(1+n^2)\Lambda}{4n} \begin{pmatrix} e^{2i\phi_1} \\ e^{2i\phi_2} \\ \vdots \\ e^{2i\phi_N} \end{pmatrix} \quad (16)$$

3.2 Case $n \neq 1$: Diagonalization and Steady-State Solution.

The stiffness matrix \mathbf{K} has the benefit of being symmetric and circulant [26]. The equations of motion (13) can be decoupled using the $(N \times N)$ Fourier matrix in the form

$$\mathbf{E}_N = \frac{1}{\sqrt{N}} \begin{pmatrix} 1 & 1 & \dots & 1 \\ W_N^1 & W_N^2 & \dots & W_N^{(N-1)} \\ \vdots & \vdots & \ddots & \vdots \\ W_N^{(N-1)} & W_N^{2(N-1)} & \dots & W_N^{(N-1)^2} \end{pmatrix} \quad (17)$$

with $W_N = e^{i(2\pi/N)}$ and the elements of Fourier matrix given by $(E_N)_{jk} = (1/\sqrt{N}) e^{i(2\pi/N)(j-1)(k-1)}$, where $j, k=1, 2, \dots, N$ [26]. The Hermitian of the Fourier matrix is given by its complex conjugate transpose and is denoted by \mathbf{E}_N^\dagger . It can be shown that $\mathbf{E}_N \cdot \mathbf{E}_N^\dagger = \mathbf{I}$ [26].

The complex amplitude vector \mathbf{U} of the order n component of the response is conveniently defined as follows:

$$\mathbf{A} = \mathbf{E}_N \mathbf{U} \quad (18)$$

Using this substitution in Eq. (13) and premultiplying the result by \mathbf{E}_N^\dagger result in the uncoupled equations for the components of \mathbf{U} given by

$$\mathbf{U}' + \tilde{\mathbf{K}}\mathbf{U} = \mathbf{E}_N^\dagger \mathbf{F} \quad (19)$$

with the diagonalized stiffness matrix:

$$\tilde{\mathbf{K}} = \mathbf{E}_N^\dagger \mathbf{K} \mathbf{E}_N = \frac{1}{2} \begin{pmatrix} \tilde{\mu}_a - in(2\sigma + \delta) & 0 & \cdots & 0 \\ 0 & \tilde{\mu}_a - 2in2\sigma & \cdots & 0 \\ \vdots & \vdots & \ddots & \vdots \\ 0 & 0 & \cdots & \tilde{\mu}_a - 2in\sigma \end{pmatrix} \quad (20)$$

The steady-state solution at order n is given by $\mathbf{A}_{ss} = \mathbf{E}_N \mathbf{U}_{ss}$ for which $\mathbf{U}'_{ss} = \mathbf{0}$. The complex amplitudes at order n for the various $n \neq 1$ cases are thus determined to be

- $n \neq 1, 2$ and any value of N : $\mathbf{A}_{ss} = \tilde{\Gamma}_\theta e^{i\tau} / (2n(\tilde{\mu}_a - in(2\sigma + \delta))) \begin{pmatrix} 1 \\ \vdots \\ 1 \end{pmatrix}$
- $n=2$ and $N=1$, $\mathbf{A}_{ss} = (\tilde{\Gamma}_\theta e^{i\tau} - i\Lambda\tilde{\gamma}(1+n^2)) / (2n(\tilde{\mu}_a - in(2\sigma + \delta)))$
- $n=2$ and $N=2$, $\mathbf{A}_{ss} = (\tilde{\Gamma}_\theta e^{i\tau} - i\Lambda\tilde{\gamma}(1+n^2)) / (2n(\tilde{\mu}_a - in(2\sigma + \delta))) \begin{pmatrix} 1 \\ 1 \end{pmatrix}$
- $n=2$ and $N>2$, $\mathbf{A}_{ss} = \tilde{\Gamma}_\theta e^{i\tau} / (2n(\tilde{\mu}_a - in(2\sigma + \delta))) \begin{pmatrix} 1 \\ \vdots \\ 1 \end{pmatrix} - (i\Lambda\tilde{\gamma}(1+n^2)) / (2n(\tilde{\mu}_a - 2in\sigma)) \begin{pmatrix} e^{2i\phi_1} \\ \vdots \\ e^{2i\phi_N} \end{pmatrix}$

The steady-state response of the j th absorber is a combination of the effects from the hard gravitational excitation and the resonant terms and at leading order can thus be approximated as follows for these separate cases (using the original θ scales here),

- $n \neq 1, 2$ and any value of N :

$$p_{jss} = \frac{\tilde{\Gamma}_\theta}{2n(\tilde{\mu}_a - in(2\sigma + \delta))} e^{i(n\theta + \tau)} + \frac{\tilde{\gamma}}{2i(n^2 - 1)} e^{i\theta_j} + c.c. \quad (21)$$

- $n=2$ and $N \leq 2$:

$$p_{jss} = \frac{\tilde{\Gamma}_\theta}{4(\tilde{\mu}_a - 2i(2\sigma + \delta))} e^{i(2\theta + \tau)} - \frac{5\tilde{\gamma}^2}{24(\tilde{\mu}_a - 2i(2\sigma + \delta))} e^{i2\theta_j} - \frac{i\tilde{\gamma}}{6} e^{i\theta_j} + c.c. \quad (22)$$

- $n=2$ and $N > 2$:

$$p_{jss} = \frac{\tilde{\Gamma}_\theta}{4(\tilde{\mu}_a - 2i(2\sigma + \delta))} e^{i(2\theta + \tau)} - \frac{5\tilde{\gamma}^2}{24(\tilde{\mu}_a - 4i\sigma)} e^{i2\theta_j} - \frac{i\tilde{\gamma}}{6} e^{i\theta_j} + c.c. \quad (23)$$

where $\theta_j = \theta + (2\pi(j-1))/N$, and in the latter two equations, we have used $n=2$ and its version of the hard excitation response amplitude, $\Lambda = -(i\tilde{\gamma}/6)$.

It is seen that in all cases the response has a component at order 1 with identical amplitude and sector phase shifts from the direct excitation due to gravity, and a component at order n with identical amplitude and equal phase from the applied torque. In the case $n \neq 1, 2$, the response is not affected by the parametric gravity effect, and thus, there are no interactions between gravity and the applied torque, and the response is a simple superposition of these two terms. For $n=2$, a case of practical importance, the gravitational parametric effects come into play and provide an additional phase-shifted component at order 2 proportional to $\tilde{\gamma}^2$. The amplitudes of the this component are slightly different depending on whether N is larger than 2, but the form of the response is the same. The key difference in the forms of the gravitational response for $N \leq 2$ and $N > 2$ is the presence of the inertia ratio δ (which is equal to unity for the present scaling) in the denominator for $N \leq 2$. This limits the response amplitude to a finite value even when the absorber is tuned exactly ($\sigma=0$) and undamped ($\tilde{\mu}_a=0$), whereas in this situation for $N > 2$, the second-order absorber amplitudes become unbounded, signaling an instability in the response that requires a nonlinear analysis.

In terms of the absorber grouping behavior, for $n \neq 1, 2$, the form of the response is just as it was assumed in Eq. (3) and thus the grouping behavior is as predicted in Table 3. For $n=2$, the order n response also depends on the relative position of the absorber, but it can be proven that in this case the grouping behavior is also as predicted.

We next turn to the case of $n=1$.

3.3 Case $n=1$. To complete the study, the case when the engine order $n=1$ must be analyzed, which corresponds to two-cylinder, four-stroke engines and one-cylinder, two-stroke engines. Here, gravity and the engine torque act at the same order and interesting interactions are expected to occur. For that purpose, it is necessary to rescale Eq. (2). By using the terms of scaling introduced in Eq. (7), the parametric terms now can be pushed out to higher order since they will have little effect when compared to the gravitational direct excitation term, which will be resonant. To this end, the scaling used is $P=L=B=Q=1/2$ and $G=\Gamma=1$, and the expansion of the EOM becomes, to leading order,

$$p_j'' + p_j + e \left[\tilde{\mu}_a p_j' + \frac{\delta}{N} \sum_{k=1}^N p_k + 2\sigma p_j - \tilde{\gamma} \sin(\theta_j) + \tilde{\Gamma}_\theta \sin(\theta + \tau) \right] = 0$$

which has no parametric excitation terms and thus is a time-invariant linear dynamical system, albeit with an interesting combination of excitation terms. From the e^0 equation, the solution for p_0 is given by $p_{0j} = A_j e^{i(\hat{\theta}_0)} + c.c.$, where A_j depends on $\hat{\theta}_1$. By replacing p_{0j} in the e^1 equation and eliminating the secular terms at first order, we find:

$$A_j' + \frac{1}{2}(\tilde{\mu}_a - 2i\sigma)A_j - i\frac{\delta}{2N} \sum_{k=1}^N A_k = \frac{1}{4}(\tilde{\Gamma}_\theta e^{i\tau} - \tilde{\gamma} e^{i\theta_j}) \quad (24)$$

This equation is similar to Eqs. (11) and (12). Following the same procedure, it is found that the form of the steady-state absorber response depends on the number of absorbers and is given by

- $n=1, N=1$:

$$p_{1ss} = \frac{\tilde{\Gamma}_\theta e^{i\tau} - \tilde{\gamma}}{2(\tilde{\mu}_a - i(2\sigma + \delta))} e^{i\theta} + c.c. \quad (25)$$

- $n=1, N > 1$:

$$p_{jss} = \frac{\tilde{\Gamma}_\theta}{2(\tilde{\mu}_a - i(2\sigma + \delta))} e^{i(\theta + \tau)} - \frac{\tilde{\gamma}}{2(\tilde{\mu}_a - 2i\sigma)} e^{i\theta_j} + c.c. \quad (26)$$

where we have combined terms in the $N=1$ result since they have common coefficients and common order. Here, the response is

simply a superposition of the direct resonant effects from the applied torque and gravity. Note that the key difference in the forms of the gravitational response for $N=1$ and $N>1$ is the presence of the inertia ratio δ (which is equal to unity for the present scaling) in the denominator for $N=1$ (similar to the $n=2$ case). This limits the response amplitude to a finite value even when the absorber is tuned exactly ($\sigma=0$) and undamped ($\tilde{\mu}_a=0$), whereas in this situation for $N>1$, the absorber amplitude again becomes unbounded, signaling an instability that requires a nonlinear analysis.

3.4 Discussion of Analytical Results. The main results for the response of the absorbers are provided by the expressions given in Eqs. (21)–(23), (25), and (26) for the cases of n and N indicated, from which one can obtain the rotor angular acceleration from Eq. (1) (for $N>1$), which is considered in Sec. 3.5.

First, note that the absorber responses have components at orders n and 1, as was assumed for the grouping results shown in Table 3. Therefore, we expect that the grouping analysis will hold for all cases, and this is indeed found to be true in numerical simulations of the EOM.

In terms of the harmonic content of the absorber response, the order n component arising from the torque is equal for all absorbers and is simply a linear, near resonant response since the absorbers are tuned close to order n . These components have equal complex amplitudes, implying they have identical magnitudes (proportional to Γ_θ) and phase.

The most straightforward case is when there are no resonances, that is, $n \neq 1, 2$. Here, the order n and 1 components of the absorber response arise directly and independently from the torque and gravity, respectively. The response in this case is simply the response predicted from linear vibration theory obtained by ignoring the parametric gravitational term. The order n response of the absorbers is proportional in amplitude to Γ_θ , and the order 1 response has amplitude proportional to γ with cyclic phases. The grouping and waveforms of the response make even these simple cases of interest.

In the resonant cases $n=1, 2$, the order n component of the absorber response contains components from both the applied torque and gravity. In these cases, the behavior of the absorbers, and their resulting effects on the rotor, can be nontrivial, as described later.

The $n=1$ case has several interesting features. Here, the response of each absorber is entirely of order 1 with terms coming from the applied torque and gravity; see Eqs. (25) and (26). The order 1 responses from gravity have amplitudes proportional to γ and cyclic phases, but their form depends on whether they are resonant ($n=1$, resonant excitation) or nonresonant ($n \neq 1$, hard excitation). For $N>1$, the gravity terms are cyclic and do not contribute to the rotor acceleration. However, for $N=1$, the single absorber will try to cancel the applied torque, but the presence of gravity results in an amplitude and phase shift of the absorber response at order 1. Here, the absorber response, in physical units, is given by $S_1 = R_0 A_1 e^{i\theta} + c.c.$. Using Eq. (25) and the attendant scaling, the nondimensional complex absorber amplitude A_1 can be expressed in terms of nondimensional physical variables as follows:

$$A_1 = \frac{\Gamma_\theta e^{i\tau} - \gamma}{2(\mu_a - i\nu)}, \quad n=1, \quad N=1 \quad (27)$$

where we have taken $\delta=1$ so that $\epsilon=\nu$ is the inertia ratio, and then ignored terms at higher order, specifically, $\delta + \sigma \approx 1$. The component proportional to Γ_θ has the correct phase for counteracting the fluctuating torque, but clearly gravity affects the absorber amplitude and phase. In this case, since there is only a single absorber, under some parameter conditions the absorber can amplify the rotor vibrations. An example of this is shown in Sec. 4. In fact, under some circumstances, e.g., $\tau=0$, there exists a torque amplitude where the absorber response is zero and it will have no effect on the rotor response to the torque.

For $n=1$ and $N>1$, the absorbers have N groups, that is, each absorber has a distinct response. Expressing the absorbers' responses in physical units as $S_j = R_0 A_j e^{i\theta} + c.c.$, using Eq. (26) and ignoring higher order terms, the nondimensional complex amplitudes of these responses are given by

$$A_j = \frac{1}{2} \left(\frac{\Gamma_\theta e^{i\tau}}{\mu_a - i\nu} - \frac{\gamma e^{i2\pi(j-1)/N}}{\mu_a} \right), \quad j=1, \dots, N, \quad n=1 \quad (28)$$

demonstrating that the amplitudes and phases depend on j . Also, note that for small damping, gravity can lead to a large response, signaling a possible instability.

The other nontrivial case is $n=2$, for which the second harmonic of the absorber response is of interest since it is a combination of the component from the torque, with amplitude proportional to Γ_θ and equal phases, and a resonant component from the parametric gravitational excitation that is proportional to γ^2 with cyclic phases. Here, we express the physical response as $S_j = R_0(A_{j,1} e^{i\theta} + A_{j,2} e^{i2\theta}) + c.c.$, using Eqs. (22) and (23). To show one of the interesting features of this harmonic, we consider the special case with $N=2$, for which the second-order harmonic coefficients have the same nondimensional complex amplitudes and are given by

$$A_{j,2} = \frac{6\Gamma_\theta e^{i\tau} - 5\gamma^2}{24(\mu_a - i2\nu)}, \quad j=1, 2; \quad n=2, \quad N=2 \quad (29)$$

which has a magnitude of

$$|A_{j,2}| = \frac{1}{24} \sqrt{\frac{25\gamma^4 - 60\gamma^2\Gamma_\theta \cos(\tau) + 36\Gamma_\theta^2}{\mu_a^2 + 4\nu^2}}, \quad (30)$$

$$j=1, 2; \quad n=2, \quad N=2$$

This result indicates that as the torque amplitude is increased from zero, the second-order harmonic amplitude can have a nonmonotonic behavior. For values of the phase τ for which $\sin\tau \geq \cos\tau \geq 0$, the magnitude has a minimum value of $5\gamma^2 \sin\tau / (24\sqrt{\mu_a^2 + 4\nu^2})$ at a critical value of $\Gamma_\theta^* = 5\gamma^2 \cos\tau / 6$, and clearly, the response experiences a phase shift as Γ_θ is varied through this value. This is demonstrated in an example in Sec. 4. This absorber behavior has an interesting effect on the rotor behavior, since at torque levels below this threshold the absorbers amplify the rotor response, while above this threshold, their phase is correct for reducing the rotor vibration. This is considered in more detail below.

The results have been described in terms of the nondimensional system and input parameters. An interesting question with practical implications is the dependence of the response on the mean rotor speed Ω . As noted in Sec. 1, this dependence is hidden by the way the parameters have been scaled, but some basic features are relatively simple to tease out of the results. The response for $n \neq 1$ consists of two harmonics, of orders 1 and n , and at most three terms, with amplitudes proportional to Γ_θ at order n , γ^2 (only for $n=2$) at order 2, and γ at order 1. Recalling that $\Gamma_\theta = T_\theta / (J_{rot}\Omega^2)$ and $\gamma = g / (R_0\Omega^2)$, it is seen that the general effects of Ω are to reduce the vibration amplitudes of the absorbers, as expected. (The consideration of $\mu_a = c_a / (M\Omega)$ is more subtle, since increasing Ω increases contact stresses and thus affects c_a .) The rotor angular acceleration similarly decreases as Ω increases, a fact well known to designers of such systems, which are most severely tested at small rotational speeds. These effects on absorber amplitude and rotor acceleration scale the same, specifically like $1/\Omega^2$, for all terms in the response except in the case $n=2$, where the term proportional to γ^2 has a stronger dependence on Ω , specifically, $1/\Omega^4$. So, as the rotor speed is increased, the order 2 effects from gravitational parametric excitation will rapidly diminish. On the other hand, at low speeds, for $n=2$, this effect may become prominent in the order 2 component of the response.

3.5 Rotor Behavior. The focus show earlier has been on the dynamics of the absorbers, but the goal of a CPVA system is to reduce the order n torsional vibrations on the rotor. Here, we consider the formulation of the rotor angular acceleration in terms of the absorber dynamics as derived earlier. As noted earlier, the present analysis describes only the order 1 and n components of the response and that higher harmonics can become prevalent in the rotor response since the absorbers generally render the order n harmonic small. More detailed investigations of the rotor vibration reduction, without considering the effects of gravity, have been considered previously [6,21,22,27,29].

To investigate the rotor behavior, we use the rotor angular acceleration given in Eq. (1), noting that $\nu = \epsilon \ll 1$ and using the scaling in Eq. (7), resulting in the following leading order expression

$$\omega' = \epsilon^2 \left(\tilde{\Gamma}_\theta \sin(n\theta + \tau) - \frac{1}{N} \sum_{j=1}^N p_j'' \right)$$

The absorber acceleration p_j'' can be expressed in terms of the corresponding leading order terms in Eq. (8) so that the rotor acceleration is given in terms of p_j , as follows:

$$\omega' = \epsilon^2 \left(\tilde{\Gamma}_\theta \sin(n\theta + \tau) + \frac{1}{N} \sum_{j=1}^N (n^2 p_j + \tilde{\gamma} \sin \theta_j) \right) \quad (31)$$

where we have retained the hard excitation term $\tilde{\gamma} \sin \theta_j$, which is valid for $n \neq 1$. However, for all values of n and $N > 1$, this gravity term will sum to zero due to the cyclic nature of the terms [26]. In fact, for $N > 1$, all terms in the summation that involve cyclic angles, including those in p_j , will sum to zero, including the order 1 terms in p_j that appear for all cases, as well as the cyclic order 2 terms that arise in the $n=2$ resonant case. This leaves only the order n terms from the torque in the summation, which are all equal. Of course, if for any reason the cyclic symmetry does not hold, for example, due to nonlinear symmetry breaking bifurcations [6], this conclusion no longer holds. Therefore, in the following discussion, our main focus is on the $N > 1$ case with cyclic symmetry, aware that for $N=1$ (a rare case in practical implementations), the gravity term will need to be retained; this case is considered below and in one of the examples provided in Sec. 4.

We can provide an expression for the rotor acceleration in terms of physical variables for $N > 1$ and any value of n by using $s_j = \epsilon p_j$, retaining only the order n component of p_j that does not involve the cyclic angle, denoted here as $s_{[n]}(\theta)$, using the fact that all such terms are equal (so that the sum is easily carried out), and replacing ϵ with ν , which yields

$$\omega' = \Gamma_\theta \sin(n\theta + \tau) + \nu n^2 s_{[n]}(\theta), \quad N > 1 \quad (32)$$

Here, the expressions for p_j in $s_j = \epsilon p_j$, used to obtain $s_{[n]}(\theta)$, are given in Eq. (21) for $n \neq 1, 2$, in Eqs. (22) and (23) for $n=2$, and Eqs. (25) and (26) for $n=1$. After determining ω' , the physical, dimensional rotor angular acceleration is given, to leading order, by $\ddot{\theta} = \Omega^2 \omega'$.

For the absorbers to be effective, the order n torque that they generate on the rotor must be (at least approximately) out of phase with respect to the applied torque so that these torques (at least partially) cancel one another. In terms of Eq. (32), this is achieved by having the applied torque term counteracted by the absorber response term. This is generally the case, but is not true in the $n=1, 2$ resonant cases at low torque levels, as demonstrated below. The effectiveness of the absorbers can then be assessed by comparing the magnitude of the order n component of the rotor angular acceleration with absorbers active with that when the absorbers are fixed at $s=0$. That is, one compares the net amplitude of the oscillation given in Eq. (32) (which is order n), with the magnitude of ω' corresponding to $s_j=0$ for all absorbers, that is, with $|\omega'|_{s=0} = \Gamma_\theta$. This comparison is considered in the literature and is not emphasized here,

except in two nontrivial examples with $n=N=1$ and $n=N=2$, as described next.

A particularly interesting case is that of a single absorber $N=1$, since in this case, the gravity terms at order 1 cannot sum to zero in Eq. (31). Here, the rotor absorber system is not dynamically balanced and will have an order 1 oscillation from gravity acting on the single absorber. Even if one statically balances the rotor with a counterweight opposite the absorber, the motion of the absorber will cause an order 1 oscillation of the rotor, even when there is no applied torque and only gravity is acting. (This is easily seen by Eq. (32), from which this situation can be addressed by taking two absorbers for which s_1 is active and $s_2 \equiv 0$ is fixed in place.) While this is true for any order n applied torque, the most interesting situation is for $N=1$ and $n=1$, for which the rotor response is entirely at order 1 (to the leading order) and is given by

$$\omega' = \Gamma_\theta \sin(\theta + \tau) + \nu s_1(\theta) + \gamma \sin \theta, \quad N=n=1 \quad (33)$$

for which we have used the special scaling of the gravity coefficient for $n=1$. In this case, which is considered in an example in Sec. 4, order 1 oscillations of the rotor are directly caused by the applied torque, gravity, and the absorber response, the latter of which is affected by both the applied torque and gravity, as indicated in Eq. (25). This results in a situation where the absorber can either attenuate or amplify the rotor response, depending on system and forcing conditions.

Similarly, in the case $n=N=2$, as noted earlier, the second-order component of the absorber response can shift phase as the torque level varies and even have zero amplitude at the crossover point. At low torque levels, the absorbers are in phase with the applied torque and thus amplify rotor vibrations. At the threshold value of the torque, derived earlier, the second-order absorber component is small (even zero) and the absorbers have no effect on the rotor. Above the threshold the absorbers function as desired, since they operate with the desired phase.

We now turn to some examples that demonstrate in more detail the more interesting features described earlier.

4 Sample Results

This section focuses on demonstrating the main features of the analytical predictions developed above. It should be noted that numerical solutions of the linear parametric EOMs given in Eq. (2) using MATHEMATICA confirm the validity of the MMS analysis for sufficiently small values of the nondimensional parameters. Typically, values of 0.05 or less for $\Gamma_\theta, \gamma, \sigma, \mu_a, \nu$, and ϵ (noting that for $\delta=1, \nu=\epsilon$) are sufficient for accurate results for the absorber and rotor responses at orders 1 and n . However, the rotor response can exhibit higher order harmonics not predicted by the present analysis [21–23]. For many cases, even larger values work quite well, but for the $n=1, N=1$ resonant case, one must keep the excitation parameters to less than ~ 0.03 for acceptable results. A comparison of the absorber responses from the analytical results and simulations of both the linear and nonlinear EOM is provided below for one of the most interesting resonant cases, $N=n=2$.

One of the main points of the results presented here are the nature of the response waveforms and how these depend on the various cases of n and N . These general observations will carry over to the nonlinear model, except when instabilities and bifurcations occur, since they are based on the dominant orders in the response, which remain valid at least into the weakly nonlinear operating regime, which for epicycloidal paths can involve relatively large absorber responses [6].

Cases with various combinations involving engine orders $n=1, 1.5, 2$ and $N=1, 2, 3, 4$ absorbers are used for the results presented in this section. These are sufficient to demonstrate the interesting features of the response and the grouping behavior, and they are the most relevant for practical applications.

Some general comments about the engine orders considered and their resonance conditions are offered before the cases are presented.

- $n = 1$, corresponding to a four-stroke, two-cylinder engine: The gravity direct excitation term is resonant and scaled at the second order, and the gravity parametric term is nonresonant and is scaled out of the present analysis. We will consider systems with $N = 1$ absorbers to demonstrate the absorber as an attenuator and an amplifier of the rotor vibration, and with $N = 3$ to show an interesting grouping and amplitude behavior.
- $n = 1.5$, corresponding to a four-stroke, three-cylinder engine: The direct excitation term from gravity is nonresonant and is scaled at the leading order and the gravity parametric term is nonresonant and is scaled out of the present analysis. For this case, we consider $N = 3$ to demonstrate a single group for a multiabsorber system.
- $n = 2$, corresponding to a four-stroke, four-cylinder engine: The direct excitation term from gravity is nonresonant and is scaled at the leading order and the gravity parametric term is resonant, scaled at the second order, and its effects are captured by the present analysis. Systems with $N = 2, 3, 4$ are considered to demonstrate various grouping behaviors and the resonant effects of gravity.

For our sample results, we consider a rotor absorber system with $R_0 = 0.1$ m spinning at mean speeds above 400 rpm, for which the nondimensionalized gravity parameter $\gamma = g/R_0\Omega^2$ ranges from very small up to a value ~ 0.05 . The torque level Γ_θ varies over a range that depends on engine load and speed conditions, and values are chosen to highlight interesting features of the response.

The damping ratio $\zeta = \mu_a/2\tilde{n} \approx \mu_a/2n$ is used to determine the damping parameter, $\mu_a = 2n\zeta$, and we take $\zeta = 0.01$, 1% of critical damping, typical for these absorbers. By taking $\delta = 1$, the system inertia ratio is given by $\nu = \epsilon = NmR_0^2/J_{rot}$, which we take to be equal to 0.0355 N, so that each individual absorber has an inertia ratio of 0.0355. The absorbers are assumed to be evenly tuned or slightly overtuned, as done in practice [6,27], with $0 \leq \sigma \leq 0.02$. We take the phase between gravity and the applied torque to be $\tau = 0$ unless otherwise specified.

The responses are plotted over a crank angle of 4π . Since $2n$ is the number of cylinders (in a four-stroke IC engine), it is always an integer, and the period of the absorber steady-state response is 2π for an even number of cylinders and 4π for an odd number of cylinders. We now consider seven cases that highlight the main results. For case 2, we provide results from numerical simulations of both the fully coupled nonlinear equations of motion for the rotor and absorbers and the linear equations of motion for the absorbers. The results from this resonant case demonstrate the validity of the linear model and the analytical predictions obtained from it. The other cases have similar agreement between theory and simulations.

Case 1: $n = 1, N = 1$. This is a special case involving a resonance and a single absorber, for which gravity directly affects the rotor response, as described earlier. Figures 2 and 3 show the steady-state response of the absorber and rotor as predicted by the theory for two levels of the torque amplitude. For the rotor response, we show the result for the absorber active ($s = s_1 \neq 0$) and the absorber locked in place ($s \equiv 0$), for which the rotor angular acceleration is given by $\omega''|_{s=0} = \Gamma_\theta \sin(\theta + \tau)$. For the larger value of torque, Fig. 2, it is seen that the absorber attenuates the rotor vibrations by about

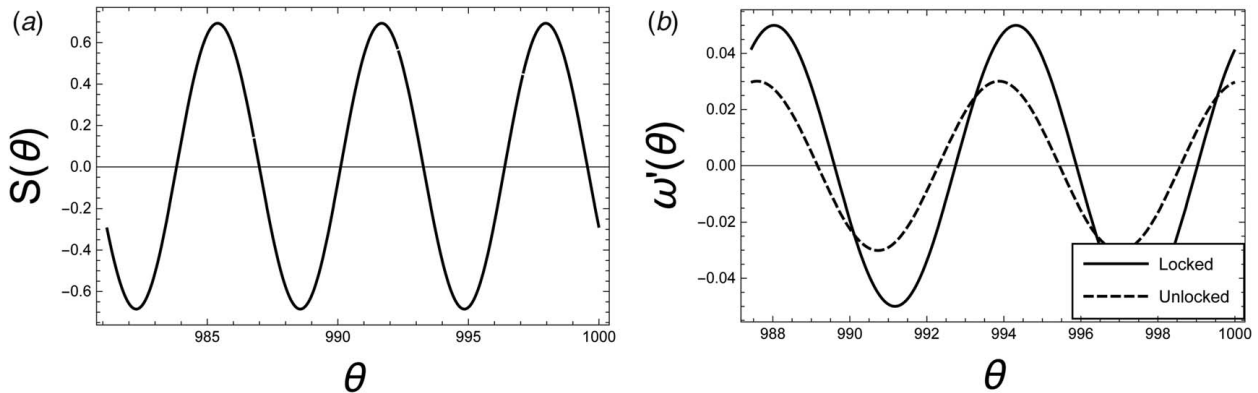


Fig. 2 Steady-state absorber response (from Eq. (25)) and rotor angular acceleration (from Eq. (33)) versus the rotor angle for $n = 1$ and $N = 1$. Parameter values: $\epsilon = 0.0355$, $\sigma = 0$, $\mu_a = 0.02$, $\tau = 0$, $\gamma = 0.02$, and $\Gamma_\theta = 0.05$. (a) Absorber response and (b) rotor response, where solid curve is for the absorber locked and the dashed curve is for the absorber active.

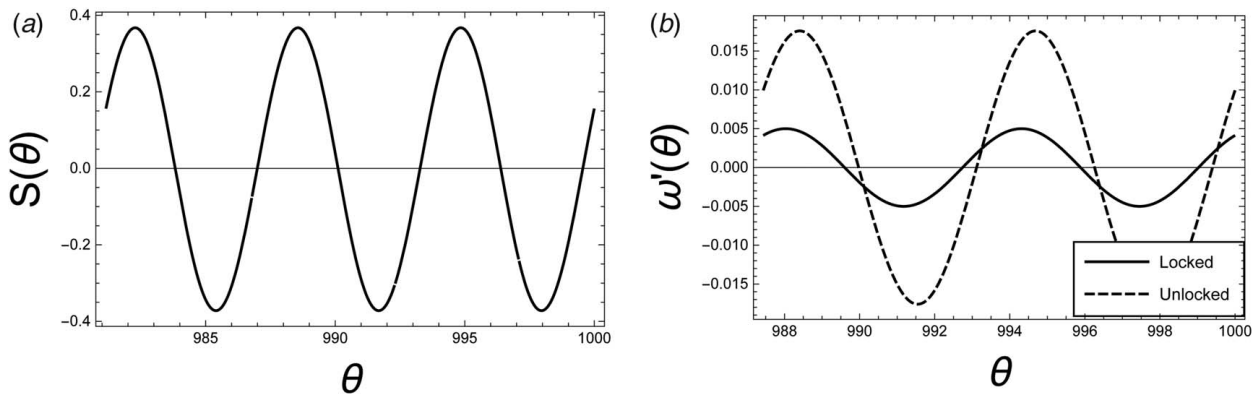


Fig. 3 Steady-state absorber response (from Eq. (25)) and rotor angular acceleration (from Eq. (33)) versus the rotor angle for the same parameter values as Fig. 2, except $\Gamma_\theta = 0.005$. (a) Absorber response and (b) rotor response.

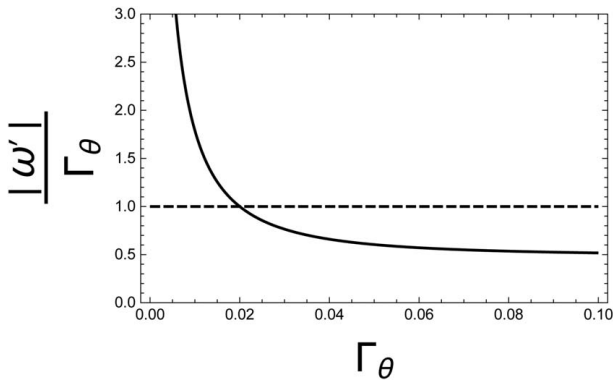


Fig. 4 Ratio of the amplitude of the rotor response with the absorber active and locked, $|\omega'|/\Gamma_\theta$, along with the attenuation/amplification boundary at unity. Parameters are those used in Fig. 2, except that Γ_θ is varied. The transition is at $\Gamma_\theta \approx 0.020$ for these parameters.

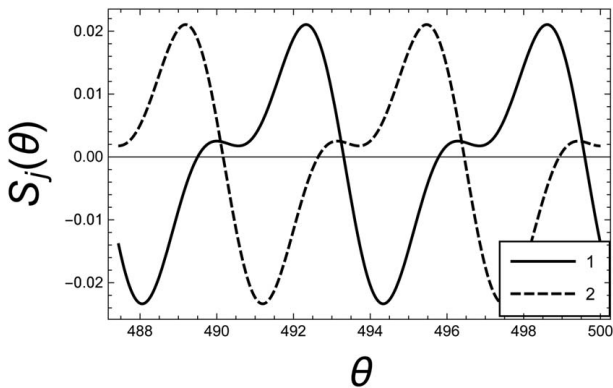


Fig. 5 Steady-state response of both absorbers versus the rotor angle for $n=2$ and $N=2$ (from Eq. (22)). Parameter values: $\epsilon = 0.071$, $\sigma = 0$, $\mu_a = 0.04$, $\tau = 0$, $\gamma = 0.05$, and $\Gamma_\theta = 0.005$.

40%, while for the smaller torque level, Fig. 3, the absorber amplifies the rotor vibration by a factor >3 . Figure 4 shows the ratio of rotor response amplitude with and without the absorber active, $|\omega'|/\Gamma_\theta$, versus the torque amplitude, for example, parameter values, indicating the range over which the absorbers amplify (>1) and attenuate (<1) the rotor response. For the example parameters, the amplification/attenuation transition occurs at $\Gamma_\theta \approx 0.020$. The amplification may not be a practical issue; however, since when the torque is relatively small, the rotor vibrations resulting from the torque are likewise small, although this will depend on the operating parameters. The “amplification” that occurs for small torque levels is a result of the fact that the gravitational component of the response persists in this case ($N=1$) and is independent of the applied torque, and when one normalizes by Γ_θ , the normalized coefficient γ/Γ_θ becomes large for small torque levels.

Case 2: $n=2$, $N=2$. For this case, there will be one group, that is, both absorbers will have identical waveforms, but shifted by the cyclic phase of π . A sample response is shown in Fig. 5, which clearly shows the shifted waveforms. In this case, the more interesting feature is the amplitude and phase of the second harmonic as a function of the torque level, which is depicted in Fig. 6. The curves are from the theoretical predictions, demonstrating the nonmonotonic nature of the second harmonic and its phase shift as it passes through the minimum value. Below the minimum point of the second harmonic, the absorbers amplify the rotor vibrations, while above this point, they perform as intended. This behavior of the rotor vibrations as the torque is varied is qualitatively

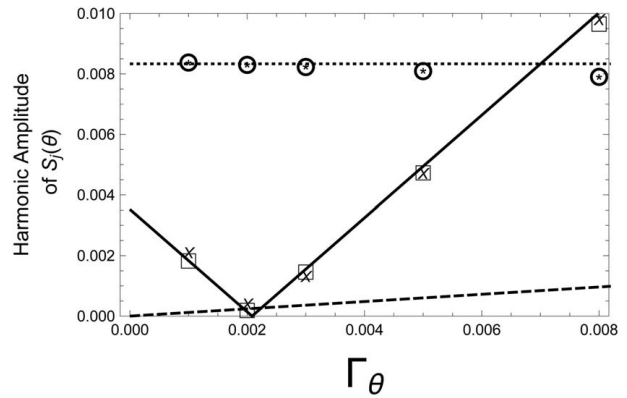


Fig. 6 Harmonic amplitudes versus torque level. The solid line is the second-order harmonic amplitude and the dotted line is the first harmonic amplitude, both with the effects of gravity, computed from Eq. (22). The dashed line is the second harmonic amplitude without gravity, $\tilde{\gamma} = 0$, from Eq. (22). Results from numerical simulations are also presented, obtained by allowing the system to settle into steady state and computing the amplitudes of the Fourier coefficients of the absorbers’ responses; open circles (*’s, respectively) are the amplitudes of the order 1 components obtained from numerical simulation of the fully nonlinear (linear, respectively) equations of motion and open squares (x’s, respectively) are the amplitudes of the order 2 components obtained from numerical simulations of the fully nonlinear (linear, respectively) equations of motion. Parameter values are the same as for Fig. 5 except that here Γ_θ is varied and $\gamma = 0$ for the case without gravity.

similar to that of case 1. Here, the crossover point, at which the absorbers have a zero second-order component, is clearly indicated in Fig. 6, and the threshold value of the torque has been derived earlier.

Also shown in Fig. 6 are results from numerical simulations of both the full nonlinear equations of motion for the absorbers and rotor and the linear absorber equations of motion, demonstrating the validity of the analytical results.

Case 3: $n=1$, $N=3$. In this case, each absorber response is dominated by its order 1 component, but there are three groups, so that each absorber has a unique waveform that is distinguished by its amplitude, as indicated by the example shown in Fig. 7. Figure 8 shows the amplitudes of the three absorbers as a function of the torque level, showing that they emerge from a non-zero value (corresponding to the amplitude due to gravity alone) and then separate rather significantly. This has implications for design, since in this

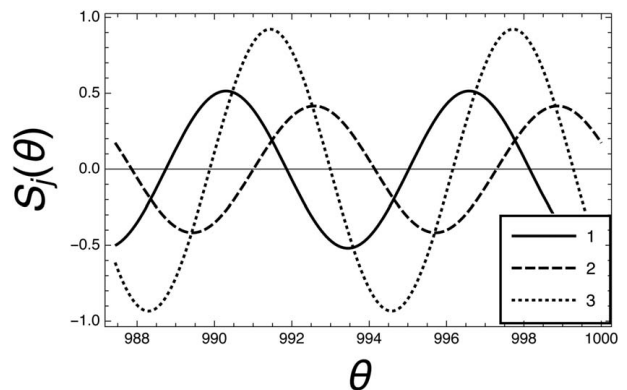


Fig. 7 Steady-state response of absorbers versus the rotor angle for $n=1$ and $N=3$ (computed using Eq. (26)). Parameter values: $\epsilon = 0.1065$, $\sigma = 0$, $\mu_a = 0.02$, $\tau = 0$, $\gamma = 0.01$, and $\Gamma_\theta = 0.05$.

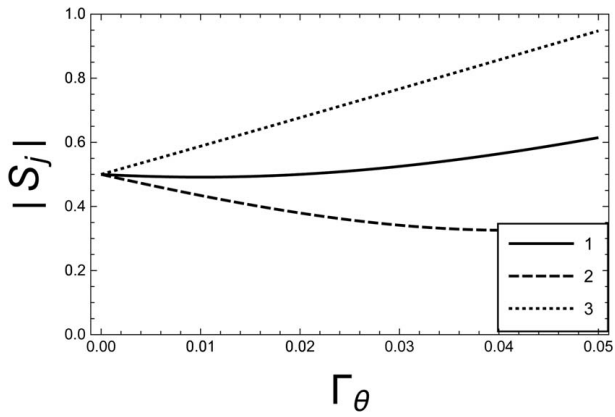


Fig. 8 Steady-state response amplitudes of the absorbers versus the torque amplitude for $n=1$ and $N=3$ (computed using Eq. (26)). Parameter values are the same as for Fig. 7 except that Γ_θ is varied.

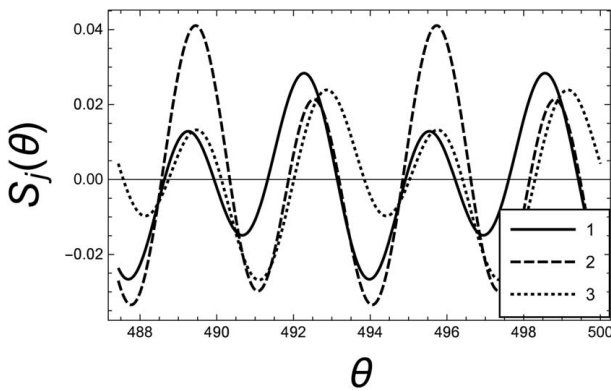


Fig. 9 Steady-state response of absorbers versus the rotor angle for $n=2$ and $N=3$ (computed using Eq. (23)). Parameter values: $\epsilon=0.1065$, $\sigma=0.02$, $\mu_a=0.04$, $\tau=0$, $\gamma=0.03$, and $\Gamma_\theta=0.01$.

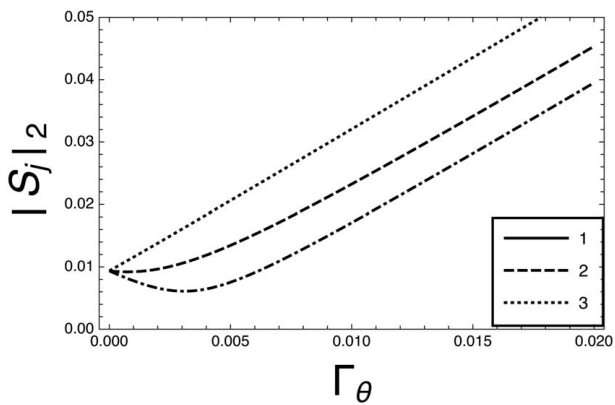


Fig. 10 Amplitudes of the second-order harmonic of the steady-state responses of the absorbers versus the torque amplitude for $n=2$ and $N=3$ (computed using Eq. (23)). Parameter values are the same as for Fig. 9 except that Γ_θ is varied.

case, the amplitude of at least one absorber is significantly increased by gravitational effects.

Case 4: $n=2$, $N=3$. In this case, there are again three groups, as indicated by the example shown in Fig. 9. The feature of interest here is that each response has harmonics at orders 1 and 2 and that here these harmonic amplitudes are relatively equal for all

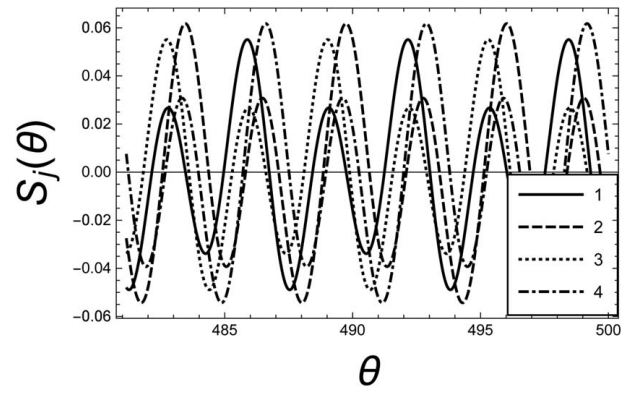


Fig. 11 Steady-state response of absorbers versus the rotor angle for $n=2$ and $N=4$ (computed using Eq. (23)). Parameter values: $\epsilon=0.142$, $\sigma=0$, $\mu_a=0.04$, $\tau=0$, $\gamma=0.05$, and $\Gamma_\theta=0.02$.

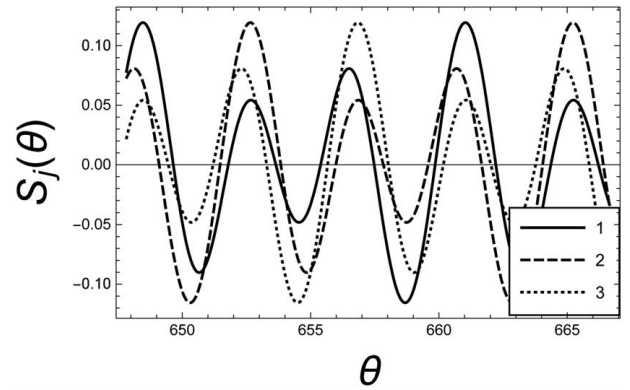


Fig. 12 Steady-state response of absorbers versus the rotor angle for $n=1.5$ and $N=3$ (computed using Eq. (21)). Parameter values: $\epsilon=0.1065$, $\sigma=0$, $\mu_a=0.03$, $\tau=0$, $\gamma=0.05$, and $\Gamma_\theta=0.02$.

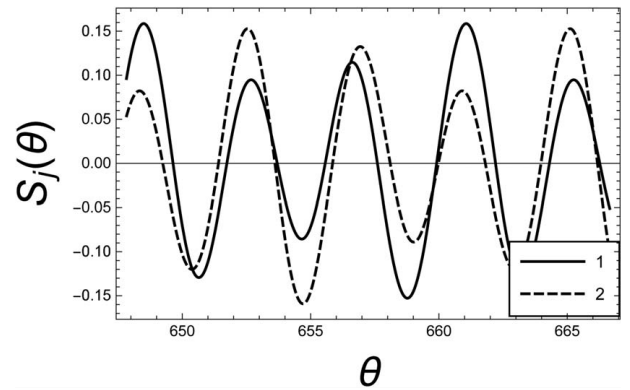


Fig. 13 Steady-state response of absorbers versus the rotor angle for $n=1.5$ and $N=2$ (computed using Eq. (21)). Parameter values: $\epsilon=0.071$, $\sigma=0$, $\mu_a=0.03$, $\tau=0$, $\gamma=0.05$, and $\Gamma_\theta=0.02$.

three absorbers for these parameter values, but their phasing leads to distinct waveforms. Figure 10 shows the amplitudes of the second-order components of the three absorbers as a function of the torque level. The amplitude of the order one components is proportional to γ and is independent of the torque level.

Case 5: $n=2$, $N=4$. This is a common arrangement of four absorbers in a four-cylinder engine. An example of this behavior is depicted in Fig. 11. In this case, there are two groups, absorbers

Table 4 Summary of grouping properties

Number of groups	Shift index	Number of absorbers per group
N	N	$\text{gcd}(a, N)$
$\text{gcd}(a, N)$	$\text{gcd}(a, N)$	

1 and 3 in one group and absorbers 2 and 4 in the other group. Again the amplitude can have nonmonotonic dependence on the torque amplitude, due to the resonant term from gravity at second-order.

Case 6: $n = 1.5, N = 3$. This is another common application, a three-cylinder engine with three absorbers. This is a nonresonant case with a single group, an example of which is shown in Fig. 12. Here, the amplitude of the absorbers monotonically increases as the torque level is increased.

Case 7: $n = 1.5, N = 2$. This is also a nonresonant case but with two groups, here implying that each absorber has a unique waveform, an example of which is shown in Fig. 13. The waveforms appear to be similar, but a close examination of the peaks reveals that they are distinct. Here, the amplitude of the absorber monotonically increases as the torque level is increased.

5 Conclusions

The results presented in this article describe the effects of gravity on rotor systems fitted with identical, cyclically arranged CPVAs. The results build and significantly expand on the preliminary results offered by Theisen [3], Shi et al. [9], and Mu [10]. The main objectives of the present effort were as follows: (i) to predict the grouping behavior of the absorbers for arbitrary numbers of CPVAs, N , and engine orders, n ; (ii) to carry out a systematic analysis of the effects of direct and parametric excitation from gravitational effects for the linearized model for all realistic values of N and n ; and (iii) finally, to investigate in detail the special cases of engine orders $n = 1, 2$ where resonance effects arise. These investigations were carried out based on a linearized mathematical model, using mathematical tools from perturbation theory and circulant matrices, for which the theoretical results were confirmed using numerical simulations.

The grouping analysis is quite general and is used to predict the waveforms of the absorbers' responses and how these organize themselves for different values of N and n . The main results are summarized in Table 3, where the numbers of groups are provided along with the phase shifts between absorbers of the same group. The present results are expected to be valid for a wide range of motions for tautochronic path absorbers, which remain essentially linear out to large amplitudes [6]. The main caveat to this observation is that systems of identical absorbers can undergo dynamic instabilities due to nonlinear coupling [4–6], and this may result in a breakdown of the present analysis; in fact, this is signaled by the singularities in the present results for very small damping and detuning. The analysis in Ref. [3] indicates that the weakly nonlinear response for systems with circular path absorbers with gravity follows the same grouping behavior (which was not analyzed in Ref. [3]), but that the absorber response curves follow a softening Duffing type behavior. This is expected, since the grouping analysis relies on the fact that the absorber response is dominated by harmonics at orders 1 and n , which will be true even for circular path absorbers.

The investigation on the effects of the gravitational parametric excitation on the system allowed us to distinguish between two main cases: the resonant cases $n = 1, 2$, where both gravity and applied torque contribute to the order n component of the absorber response, and the nonresonant cases $n \neq 1, 2$, where the effects of

the applied torque and gravity are independent. The present results offer approximate analytical expressions for the steady-states responses that match the general form assumed for the grouping analysis, which holds for all values of N and n , and match numerical simulations of the full model EOM.

For the resonant cases, one can determine the conditions on physical parameters at which the absorber motions have roughly equal components from the applied torque and gravity. Based on the analytical results, it is seen that for order 1, this condition is given by $\Gamma_\theta/\gamma \sim 1$, which translates to $T_0 R_0/J_{rot} g \sim 1$. For order 2, this condition is given by $\Gamma_\theta/\gamma^2 \sim 1$ which translates to $T_0 R_0^2 \Omega^2/J_{rot} g^2 \sim 1$. The absorbers will function with the correct phase only when the applied torque is sufficiently large so that these ratios are significantly larger than unity.

The response of the rotor, which is the ultimate goal of the CPVA system, can be compared to the response with the absorbers locked. The absorbers, in the absence of gravity and if properly tuned, generally reduce the amplitude of rotor vibration. However, when gravity acts on the system, as seen herein, for the resonant cases $n = 1, 2$, the absorber amplitudes and phases have a complicated dependence on the ratio Γ_θ/γ^n . In these cases, at relatively small torque amplitudes, the absorbers can amplify the rotor vibrations, but at larger torque amplitudes, the absorbers perform as desired. The importance of these effects will depend on the specific system parameters and operating conditions.

Generally, for $N > 1$, except in the resonant case $n = N = 2$, the cyclic nature of the absorber response due to gravity results in their net cancellation in the rotor response, so that previous work on CPVAs generally carries over. Specifically, except for the cases $N = 1$ and $n = N = 2$, gravity does not affect the response of the rotor to the present level of analysis, even though gravity has a significant effect on the response of the absorbers. However, for a single absorber ($N = 1$), there is no such cancellation and the gravity term directly affects the rotor response. For $n \neq 1, N = 1$, the effects from gravity and the torque are independent, since they are at different orders. However, for $n = 1, N = 1$, the effects combine and can result in amplification of the rotor vibrations, as described in case 1 in Sec. 4. For $n = N = 2$, the resonance causes gravity to affect the second-order absorber response and results in its non-monotonic amplitude as the torque is varied, and the attendant nonmonotonic effect on the rotor response, as described in case 2 in Sec. 4.

Note that this study does not give specific information about the stability of the response, which is of particular interest in the resonant cases $n = 1, 2$. The possibilities for instabilities are indicated in cases where the response predicted by this linear analysis can become unbounded for small detuning and damping. To extend the present analysis, it would be necessary to investigate nonlinear system models with gravity, along the lines of the preliminary study of Theisen [3]. This would provide stability information about the response and would also provide important information about the higher order harmonic components in the rotor response [21,22]. In addition, future work on this topic should include experimental verification of the analytical predictions provided by the present study (see Table 4).

Acknowledgment

The authors would like to thank Tom Theisen, Rob Parker, and Chengzhi Shi for technical discussions that contributed to this study, and Cody Clemons for help with preparation of the manuscript. S. W. S. efforts are supported in part by NSF (Grant No. CMMI-1662619).

Conflict of Interest

There are no conflicts of interest.

Data Availability Statement

The authors attest that all data for this study are included in the paper.

Appendix

Grouping Behavior Proof. Given the general structure of possible steady-state solutions derived in Secs. 3.2 and 3.3 for N equally spaced absorbers on a rotor subjected to an order n excitation and gravity, a question arises: Which absorbers can belong to a subgroup where each member of the subgroup has an identical, phase-shifted response to any other absorber in the subgroup? To address this question, a smallest shift index ℓ is identified such that, if possible, $s_j(\theta + \psi) = s_{j+\ell}(\theta)$ for some angle $\psi \in (0, 2\pi)$. Upon identifying this smallest index ℓ , every ℓ th absorber counting from absorber j along the rotor belongs to a subgroup that includes the j th absorber. The proof below will demonstrate that the index ℓ divides N (the number of absorbers) evenly, as it must, so that the number of absorbers per subgroup is N/ℓ .

The template steady-state solution indicated in Eq. (A1) of Lemma 1 represents all possible steady-state solutions cases. Choices for absorber amplitude coefficients A , B , and C , and phase angles ρ_A , ρ_B , and ρ_C are case dependent. The steady-state response of the j th absorber in the case where engine order $n \neq 1, 2$ is identified in Eq. (21) (and so $B=0$ in this case). When $n=2$, Eqs. (22) and (23) identify the steady-state response when the number of absorbers $N \leq 2$ and $N > 2$, respectively. On the other hand, for $n=1$, Eqs. (25) and (26) give the steady-state solution for the cases for $N=1$ and $N > 1$, respectively. Without loss of generality, the coefficients A , B , and C can be assumed real, because if they are complex, phase angles ρ_A , ρ_B , and ρ_C can be adjusted to create an equivalent expression where A , B , or C are positive real values. The absorber vibration amplitudes are $2A$, $2B$, and $2C$ because the complex conjugate of each exponential term is added back as part of the templated solution. For the derivations in this Appendix, the specific values of A , B , and C are unimportant, because the investigation here centers on when a phase angle shift ψ is mathematically possible for a given modeling scenario defined by the values for N and n ; the amplitudes are unimportant for determining when this can be so. Likewise, the actual constant values of ρ_A , ρ_B , and ρ_C are not important, as these variables fall away from simplified congruencies that identify when a phase angle ψ exists such that Eq. (A3) can be satisfied. Of course, the nature of the waveforms in each group depend on these amplitudes and phases, and expressions for these are provided in this article.

Concepts and notation from elementary number theory facilitate the proofs that follow. Specifically, an integer p is said to divide integer q if and only if there is a positive integer c such that q can be written as $q=c \cdot p$. The notation for indicating that p divides q is follows:

$$p|q$$

Two integers p and q are said to be relatively prime if the only positive integer that divides both p and q is 1. For example, $p=21$ and $q=10$ are relatively prime, because the only positive integer divisor shared by both p and q is 1. Also, the greatest common divisor of two integers p and q is denoted by

$$\gcd(p, q)$$

and is defined to be the largest positive integer that divides both p and q . For $p=21$ and $q=10$, the greatest common divisor is $\gcd(21, 10)=1$. On the other hand, $\gcd(21, 15)=3$. Finally, as usual, we denote the set of integers by \mathbb{Z} .

The Lemmas and Theorem below assume order n to be a proper fraction a/b . That is, $n=a/b$ where integers a and b have a greatest common divisor of 1: $\gcd(a, b)=1$. For four-stroke internal combustion engines with an even number of cylinders, $b=1$ and a is half the number of cylinders. For four-stroke internal combustion

engines with an odd number of cylinders, $b=2$ and a is the number of cylinders. For some technologies available today (for example, dynamic skip fire where cylinder firing densities can be prescribed), more exotic engine orders are possible, but always in the form of a rational number $n=a/b$.

LEMMA 1. Let engine order $n=a/b$, where a and b are relatively prime integers (no common prime factors). Suppose there are N absorbers, and that $N \geq 2$. Let integer ℓ be selected from $\{1, 2, \dots, N-1\}$. Define $f=\gcd(a, N)$, and let $a_1=af$ and $N_1=N/f$ (so that a_1 and N_1 are relatively prime). The general steady-state form of the j th absorber can be expressed as follows:

$$s_j(\theta) = Ae^{i(n\theta + \rho_A)} + Be^{i(n\theta_j + \rho_B)} + Ce^{i(\theta_j + \rho_C)} + \text{c.c.} \quad (\text{A1})$$

where A , B , and C can be considered positive real coefficients; ρ_A , ρ_B , and ρ_C allow for phase differences between harmonic components; c.c. denotes the complex conjugate of the preceding terms; and $\theta_j = \theta + (2\pi(j-1))/N$. Let $k=j+\ell$ (so that absorber k is an absorber ℓ circumferential sections from absorber j), and define

$$s_k(\theta) = Ae^{i(n\theta + \rho_A)} + Be^{i(n\theta_j + n\frac{2\pi\ell}{N} + \rho_B)} + Ce^{i(\theta_j + \frac{2\pi\ell}{N} + \rho_C)} + \text{c.c.} \quad (\text{A2})$$

Then, there exists a phase angle shift ψ such that

$$s_j(\theta + \psi) = s_k(\theta) \quad (\text{A3})$$

if and only if there is an integer q such that

$$bN_1 | (\ell + Nq) \quad (\text{A4})$$

Proof. The condition that $s_j(\theta + \psi) = s_k(\theta)$ implies that

$$n\psi \equiv 0 \pmod{2\pi} \quad (\text{A5})$$

$$\theta_j + \frac{2\pi\ell}{N} \equiv \theta_j + \psi \pmod{2\pi} \quad (\text{A6})$$

Congruence (A5) holds if and only if there exists an integer p such that

$$n \cdot \frac{\psi}{2\pi} = p \quad (\text{A7})$$

Congruence (A6) holds if and only if there exists an integer q such that

$$\frac{2\pi\ell}{N} = \psi - 2\pi \cdot q$$

which holds if and only if

$$\frac{\ell}{N} = \frac{\psi}{2\pi} - q \quad (\text{A8})$$

It follows that a phase angle ψ exists if and only if there exist integers p and q such that

$$\left(\frac{\ell}{N} + q\right)n = p \quad (\text{A9})$$

Equation (A9) holds if and only if

$$\begin{aligned} (\ell + Nq)\frac{n}{N} &\in \mathbb{Z} \\ \Leftrightarrow (\ell + Nq) \cdot \frac{a}{b} \cdot \frac{1}{N} &\in \mathbb{Z} \\ \Leftrightarrow (\ell + Nq) \cdot \frac{af}{bN_1f} &\in \mathbb{Z} \\ \Leftrightarrow (\ell + Nq) \cdot \frac{a_1}{bN_1} &\in \mathbb{Z} \end{aligned} \quad (\text{A10})$$

Because bN_1 has no common factors with a_1 , relation (A10) can be true if and only if $bN_1 | (\ell + Nq)$. ■

LEMMA 2. Let ℓ, f, q , and N_1 be defined as in the previous lemma. Suppose that $bN_1 | (\ell + Nq)$. Then, $N_1 | \ell$.

Proof. This is an immediate consequence of the hypothesis that $bN_1 | (\ell + Nq)$. To demonstrate that N_1 must divide ℓ , observe that $\ell + N_1 f q = cbN_1$ if and only if

$$\begin{aligned}\ell &= cbN_1 - N_1 f q \\ &= (cb - qf)N_1\end{aligned}$$

$\ell \in \{1, 2, \dots, N-1\}$, so $\ell \geq 1$, which implies the integer coefficient $cb - qf \geq 1$, which implies that $N_1 | \ell$. ■

THEOREM 1. Let $f, N_1, n = alb$, and N be defined as in Lemma 1. Let $f > 1$, so that $N_1 = N/f < N$. Then, $\ell = N_1 \in \{1, 2, \dots, N-1\}$ is the smallest shift index for which there is a phase angle shift ψ so that Eq. (A3) is satisfied. Shift index N_1 corresponds to a phase angle satisfying

$$\psi \equiv \frac{2\pi}{f} \pmod{2\pi} \quad (\text{A11})$$

Proof. Because $\gcd(a, b) = \gcd(a \cdot f, b) = 1$, it follows that $\gcd(f, b) = 1$. Bezout's identity³ can be applied to conclude that there exist integers q' and c' such that

$$\gcd(b, f) = 1 = c'b - q'f \quad (\text{A12})$$

Multiplying the last equation through by N_1 , it follows that

$$N_1 + q'N_1 f = c'bN_1 \quad (\text{A13})$$

This implies that $bN_1 | (N_1 + q'N_1 f)$. Then, Lemma 1 shows that N_1 is a shift index for which a phase angle ψ exists such that Eq. (A3) holds. The previous Lemma shows that N_1 always divides a shift index; hence, N_1 is the smallest shift index possible for which a phase angle ψ exists such that Eq. (A3) holds. Congruence (A11) follows from Eq. (A6) when $\ell = N_1$. ■

Remarks. Lemma 2 implies that if $f=1$, and hence that $N_1=N$, there is no shift index $\ell \in \{1, 2, \dots, N-1\}$; in this case, every absorber has a unique waveform. For $f \geq 2$, when $\ell = dN_1$, where $d \in \{1, 2, \dots, f-1\}$, Eq. (A13) can be multiplied through by d to show that $dbN_1 | (dN_1 + d q' N_1 f)$, which shows that there exists a ψ such that $s_j(\theta + \psi) = s_{(j+dN_1) \pmod{N}}(\theta)$.

The parameter ℓ is a generator of an additive subgroup within the additive group Z_N . (Z_N is the group of integers with addition modulo N as the group operation.) Starting at an index $k \in Z_N$, and repeatedly adding ℓ using addition modulo N , generates a subgroup of indexes in $Z_N = \{0, 1, \dots, N-1\}$, where each element of the subgroup identifies a single absorber along the rotor. The order of element $\ell \in Z_N$ defines the cardinality of the subgroup, and hence, the number of absorbers in the subgroup, all of which have identical but phase-shifted responses.

The results of Theorem 1 can be used to express the information in Table 3 in a more rigorous, abstract, and compact manner.

References

- [1] Reese, R., 2015, "A Multi-air/Multifuel Approach to Enhancing Engine System Efficiency, US Department of Energy FCA US LLC (formerly "Chrysler Group LLC"), Technical Report OSTI Identifier 1228747, <https://www.osti.gov/biblio/1228747>, pp. 23–24.
- [2] Wellmann, T., Govindswamy, K., and Tomazic, D., 2017, "Impact of the Future Fuel Economy Targets on Powertrain, Driveline and Vehicle NVH Development," *SAE Int. J. Veh. Dyn., Stab., and NVH*, **1**(2), pp. 428–438.

³Bezout's identity states that for integers u and v with $\gcd(u, v) = d$, there exist integer coefficients x and y such that $x \cdot u + y \cdot v = d$. Bezout's identity applied here shows that for integers b and f with $\gcd(b, f) = 1$, there exist integers c' and q' such that $1 = c'b - q'f$. The negative sign in front of q' is taken for convenience, to avoid carrying a negative sign in front of q' in subsequent formulas. Bezout coefficients c' and q' can be calculated using the extended Euclidean Algorithm as explained in Ref. [30].

- [3] Theisen, T., 2012, "Gravity's Effect on Centrifugal Pendulum Vibration Absorbers," M.S. thesis, Department of Mechanical Engineering, Michigan State University, East Lansing, MI.
- [4] Chao, C.-P., Lee, C.-T., and Shaw, S., 1997, "Non-Unison Dynamics of Multiple Centrifugal Pendulum Vibration Absorbers," *J. Sound. Vib.*, **204**(5), pp. 769–794.
- [5] Alsuwaiyan, A. S., and Shaw, S. W., 2002, "Performance and Dynamic Stability of General-Path Centrifugal Pendulum Vibration Absorbers," *J. Sound. Vib.*, **252**(5), pp. 791–815.
- [6] Shaw, S. W., and Geist, B., 2010, "Tuning for Performance and Stability in Systems of Nearly Tautochronic Torsional Vibration Absorbers," *ASME J. Vib. Acoust.*, **132**(4), p. 041005.
- [7] Ulbrich, H., and Mayet, J., 2018, "Centrifugal Pendulum," Mar. 13, US Patent 9,915,317.
- [8] Maienschein, S., 2019, "Centrifugal Pendulum," Oct. 15, US Patent 10,443,682.
- [9] Shi, C., Parker, R. G., and Shaw, S. W., 2014, "Vibration Response of Rotor Systems With Centrifugal Pendulum Vibration Absorbers Under Gravitational Loading," 15th International Symposium on Transport Phenomena and Dynamics of Rotating Machinery, ISROMAC-15, Honolulu, HI, Feb. 24–28.
- [10] Mu, M., 2015, "Gravitation Effects on Centrifugal Pendulum Vibration Absorbers, Linear Analysis," M.S. thesis, Department of Mechanical Engineering, Michigan State University, East Lansing, MI.
- [11] Rugar, D., and Grütter, P., 1991, "Mechanical Parametric Amplification and Thermomechanical Noise Squeezing," *Phys. Rev. Lett.*, **67**(6), p. 699.
- [12] Rhoads, J. F., Miller, N. J., Shaw, S. W., and Feeny, B. F., 2008, "Mechanical Domain Parametric Amplification," *ASME J. Vib. Acoust.*, **130**(6), p. 061006.
- [13] Acar, G. D., Acar, M. A., and Feeny, B. F., 2020, "Parametric Resonances of a Three-Blade-Rotor System With Reference to Wind Turbines," *ASME J. Vib. Acoust.*, **142**(2), p. 021013.
- [14] Sapmaz, A., Acar, G. D., and Feeny, B. F., 2017, "In-Plane Blade-Hub Dynamics of Horizontal-Axis Wind Turbines With Mistuned Blades," ASME International Design Engineering Technical Conferences and Computers and Information in Engineering Conference, Cleveland, OH, Aug. 6–9, Paper No. IDETC2017-67687.
- [15] Sapmaz, A., and Feeny, B. F., 2018, "Second-Order Perturbation Analysis of In-Plane Blade-Hub Dynamics of Horizontal-Axis Wind Turbines," ASME International Design Engineering Technical Conferences and Computers and Information in Engineering Conference, Quebec City, Montreal, CA, Aug. 26–29, Paper No. IDETC2018-88203.
- [16] Sapmaz, A., and Feeny, B. F., 2020, "Parametric Stiffness in Large-Scale Wind-Turbine Blades and the Effects on Resonance and Speed Locking," ASME International Design Engineering Technical Conferences and Computers and Information in Engineering Conference, Aug. 17–19, Paper No. IDETC2020-27717.
- [17] Ikeda, T., Harata, Y., and Ishida, Y., 2018, "Parametric Instability and Localization of Vibrations in Three-Blade Wind Turbines," *ASME J. Comput. Nonlinear. Dyn.*, **13**(7), p. 071001.
- [18] Ramakrishnan, V., 2017, "Analysis of Wind Turbine Blade Vibration and Drivetrain Loads," Ph.D. thesis, Michigan State University, East Lansing, MI.
- [19] Ramakrishnan, V., and Feeny, B. F., 2012, "Resonances of the Forced Mathieu Equation With Reference to Wind Turbine Blades," *ASME J. Vib. Acoust.*, **134**(6), p. 064501.
- [20] Inoue, T., Ishida, Y., and Kiyohara, T., 2012, "Nonlinear Vibration Analysis of the Wind Turbine Blade (Occurrence of the Superharmonic Resonance in the Out-of-Plane Vibration of the Elastic Blade)," *ASME J. Vib. Acoust.*, **134**(3), p. 031009.
- [21] Lee, C.-T., and Shaw, S., 1996, "On the Counteraction of Periodic Torques for Rotating Systems Using Centrifugally Driven Vibration Absorbers," *J. Sound. Vib.*, **191**(5), pp. 695–719.
- [22] Vidmar, B. J., Shaw, S. W., Feeny, B. F., and Geist, B. K., 2013, "Nonlinear Interactions in Systems of Multiple Order Centrifugal Pendulum Vibration Absorbers," *ASME J. Vib. Acoust.*, **135**(6), p. 061012.
- [23] Vidmar, B. J., Shaw, S. W., Feeny, B. F., and Geist, B. K., 2012, "Analysis and Design of Multiple Order Centrifugal Pendulum Vibration Absorbers," ASME International Design Engineering Technical Conferences and Computers and Information in Engineering Conference, Chicago, IL, Aug. 12–15, American Society of Mechanical Engineers, pp. 165–173.
- [24] Denman, H., 1992, "Tautochronic Bifilar Pendulum Torsion Absorbers for Reciprocating Engines," *J. Sound. Vib.*, **159**(2), pp. 251–277.
- [25] Alsuwaiyan, A., and Shaw, S. W., 2003, "Steady-State Responses in Systems of Nearly-Identical Torsional Vibration Absorbers," *ASME J. Vib. Acoust.*, **125**(1), pp. 80–87.
- [26] Olson, B. J., Shaw, S. W., Shi, C., Pierre, C., and Parker, R. G., 2014, "Circulant Matrices and Their Application to Vibration Analysis," *ASME Appl. Mech. Rev.*, **66**(4), p. 040803.
- [27] Newland, D. E., 1964, "Nonlinear Aspects of the Performance of Centrifugal Pendulum Vibration Absorbers," *ASME J. Manuf. Sci. Eng.*, **86**(3), pp. 257–263.
- [28] Nayfeh, A., and Mook, D., 2008, *Nonlinear Oscillations*, Wiley Classics Library, Wiley.
- [29] Wilson, W., 1965, "Practical Solution of Torsional Vibration Problems With Examples From Marine Electrical Aeronautical and Automobile Engineering Practice," No. v. 3 in Practical Solution of Torsional Vibration Problems With Examples From Marine Electrical Aeronautical and Automobile Engineering Practice, Wiley.
- [30] Burton, D. M., 2007, *Elementary Number Theory*, 6th ed., McGraw-Hill, New York.